

Aporphine and Tetrahydroprotoberberine Alkaloids from the Leaves of *Guatteria friesiana* (Annonaceae) and their Cytotoxic Activities

Emmanoel Vilaça Costa,^{*,a,b} Pedro Ernesto O. da Cruz,^a Maria Lúcia B. Pinheiro,^c
Francisco A. Marques,^b Ana Lúcia T. G. Ruiz,^d Gabriela M. Marchetti,^d
João Ernesto de Carvalho,^d Andersson Barison^b and Beatriz Helena L. N. S. Maia^b

^aDepartamento de Química, Universidade Federal de Sergipe,
Av. Marechal Rondon, s/n, Rosa Elze, 49100-000 São Cristovão-SE, Brazil

^bDepartamento de Química, Universidade Federal do Paraná, Centro Politécnico,
Jardim das Américas, 81531-990 Curitiba-PR, Brazil

^cDepartamento de Química, Universidade Federal do Amazonas, Mini-Campus,
Av. General Rodrigo Otávio Jordão Ramos, 3000, Coroado, 69077-000 Manaus-AM, Brazil

^dDivisão de Farmacologia e Toxicologia, Centro Pluridisciplinar de Pesquisas Químicas, Biológicas e Agrícolas,
Universidade Estadual de Campinas, 13083-970 Campinas-SP, Brazil

A investigação fitoquímica das folhas de *Guatteria friesiana* (Annonaceae) levou à obtenção de três novos alcaloides isoquinolínicos, 13-hidroxi-discretinina, 6,6a-desidroguateriopsiscina e 9-desidroxí-1-metoxi-diidroguatouregidina, juntamente com oito alcaloides conhecidos, 13-hidroxi-2,3,9,10-tetrametoxiprotoberberina, guateriopsiscina, liscamina, lirioidenina, aterospermidina, lanuginosina, 7,8-diidro-8-hidroxipalmatina e palmatina. 13-Hidroxi-2,3,9,10-tetrametoxiprotoberberina, obtido somente através de síntese, é relatada pela primeira vez como produto natural. As estruturas dos alcaloides isolados foram elucidadas por extensivas análises de ressonância magnética nuclear (RMN 1D e 2D), espectrometria de massas (MS) e comparação com os dados descritos na literatura. A atividade citotóxica *in vitro* dos alcaloides majoritários foi avaliada frente a linhagens de células tumorais e não tumorais. Considerando a atividade média, de acordo com os critérios do National Cancer Institute (NCI/EUA), todos os alcaloides avaliados foram inativos. Entretanto, o alcaloide palmatina apresentou efeito citostático para as linhagens MCF-7 (mama) e U251 (glioma) com valores de GI₅₀ abaixo de 20,0 μmol L⁻¹ (10,5 e 16,2 μmol L⁻¹, respectivamente), sugerindo uma ação citotóxica seletiva.

Phytochemical investigation of the leaves of *Guatteria friesiana* (Annonaceae) afforded three new isoquinoline alkaloids, 13-hydroxy-discretinine, 6,6a-dehydroguateriopsiscine and 9-dehydroxy-1-methoxy-dihydroguatouregidine. Eight known alkaloids were also isolated, 13-hydroxy-2,3,9,10-tetramethoxyprotoberberine, guateriopsiscine, lysicamine, lirioidenine, atherospermidine, lanuginosine, 7,8-dihydro-8-hydroxypalmatine and palmatine. 13-Hydroxy-2,3,9,10-tetramethoxyprotoberberine was only obtained by synthesis and is being reported as a natural product for the first time. The structures of the isolated alkaloids were established by extensive analysis of 1D and 2D nuclear magnetic resonance (NMR) and mass spectrometric (MS) data, as well as by comparison with data reported in the literature. The *in vitro* cytotoxic activity of the major alkaloids was evaluated against tumor and non-tumor cell lines. All of the alkaloids evaluated were determined to be inactive based on National Cancer Institute (NCI/USA) criteria. However, the alkaloid palmatine exhibited a cytostatic effect on MCF-7 (breast) and U251 (glioma) human tumor cell lines, with GI₅₀ values lower than 20.0 μmol L⁻¹ (10.5 and 16.2 μmol L⁻¹, respectively), suggesting a selective cytotoxic action.

Keywords: *Guatteria friesiana*, aporphine alkaloids, tetrahydroprotoberberine alkaloids, cytotoxic activity

Introduction

The genus *Guatteria* (Ruiz & Pav.) is the largest in the family Annonaceae and comprises approximately 210 recognized species, distributed exclusively in the Neotropical regions (although not in Argentina and Paraguay).^{1,2} Some species of this genus are known for their aromatic fragrances and their medicinal properties.³ Previous phytochemical and pharmacological investigations on some *Guatteria* species revealed the presence of bioactive compounds, including cytotoxicity against human tumor cell lines,⁴⁻⁶ as well as antimicrobial,^{4,5,7-10} antioxidant⁷ and antiparasitic activity against *Leishmania* sp.,^{11,12} *Plasmodium falciparum*¹² and *Trypanosoma cruzi*.¹² These bioactivities are attributed to the presence of terpenes and alkaloids in these plant species. *Guatteria friesiana* (W. A. Rodrigues) Erkens & Maas is a small tree known as both “envreira” and “envira” found in the Brazilian and Colombian Amazon Basin. Previous phytochemical investigations on this species described the chemical constituents of its essential oils,^{6,9,13} as well as aporphine alkaloids.⁸ The alkaloids and essential oils exhibited antitumor and antimicrobial properties,^{4,6-9} as well as larvicidal activity against *Aedes aegypti* larvae.¹³

In our continuous search for bioactive compounds from Amazonian annonaceous plants, three new (**1**, **3**, **4**) and eight known (**2**, **5-11**) alkaloids (Figure 1) were obtained in a systematic bio-guided investigation of the leaves of *G. friesiana*. Their structures were established based

on spectrometric data, including 1D and 2D NMR experiments, as well as 1D nuclear Overhauser effect (NOE) and high-resolution mass spectrometry (HRMS) analyses. Some *in vitro* cytotoxic activities against tumor cell lines were demonstrated for the pure compounds.

Experimental

General

UV spectra were obtained in CH₃OH on an Agilent HP 8453 UV-Vis spectrophotometer. IR spectra were acquired in KBr pellets on a BIORAD FTS-3500 GX spectrophotometer. Optical rotations were measured in CHCl₃ or MeOH solutions at room temperature on a Rudolph Research Autopol III automatic polarimeter. Circular dichroism analyses were measured in MeOH on a JASCO J-720 spectropolarimeter. 1D and 2D NMR experiments were acquired in CDCl₃, CDCl₃ + drops of CD₃OD, or CD₃OD at 293 K on a Bruker AVANCE 400 NMR spectrometer operating at 9.4 T, observing ¹H and ¹³C at 400 and 100 MHz, respectively. The spectrometer was equipped with a 5 mm multinuclear direct detection probe with z -gradient. One-bond (HSQC) and long-range (HMBC) ¹H-¹³C NMR correlation experiments were optimized for average coupling constants ¹J_(C,H) and ¹RJ_(C,H) of 140 and 8 Hz, respectively. All ¹H and ¹³C NMR chemical shifts (δ) are given in ppm relative to the tetramethylsilane (TMS) signal at 0.00 ppm as internal reference, and the coupling

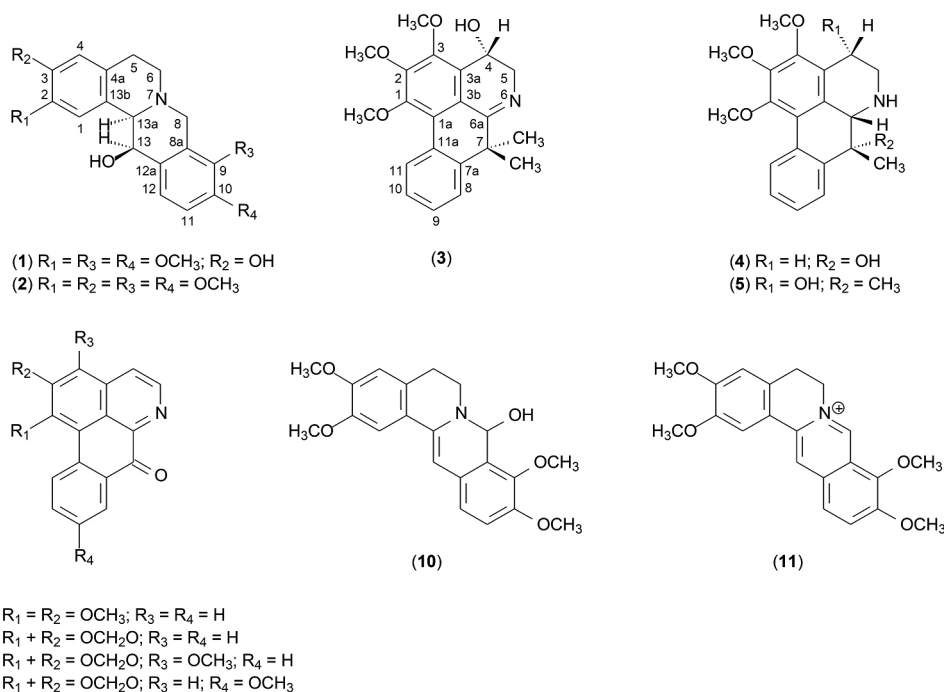


Figure 1. Aporphine and tetrahydroprotoberberine alkaloids isolated from the leaves of *Guatteria friesiana* (Annonaceae).

constants (J) are given in Hz. HRESIMS measurements were performed on a Bruker UltratOF-Q MS spectrometer featuring a quadrupole time-of-flight mass analyzer equipped with an electrospray source. Silica gel 60 (70-230 mesh) was used for column chromatography, while silica gel 60 F₂₅₄ was used for analytical (0.25 mm) and preparative (1.00 mm) thin layer chromatography (TLC). Compounds were visualized by exposure under UV_{254/365} light, by spraying with *p*-anisaldehyde reagent followed by heating on a hot plate, and by spraying with Dragendorff's reagent.

Plant material

The leaves from flowered plants of *Guatteria friesiana* were collected in January 2005 on the experimental farm of the Amazonas Federal University (UFAM) (Manaus City, Amazonas State, Brazil), and identified by the taxonomist Prof. Dr. A. C. Webber from UFAM. A voucher specimen (No. 7341) was deposited in the Herbarium of the UFAM.

Extraction and isolation

Leaves of *G. friesiana* (1300 g) were dried at room temperature, powdered and successively extracted with *n*-hexane followed by MeOH to yield *n*-hexane (77.64 g) and MeOH (215.80 g) extracts. TLC analysis indicated a high concentration of alkaloids in the MeOH extract. Therefore, an aliquot of the MeOH extract (210.0 g) was initially subjected to acid-base extraction to give CH₂Cl₂ alkaloid (4.5 g) and CH₂Cl₂ neutral (30.0 g) fractions.¹⁴ The alkaloid fraction (4.0 g) was subjected to column chromatography on silica gel treated with 10% NaHCO₃.¹⁴ The column was eluted with gradient systems (petroleum ether:CH₂Cl₂ from 100:0 to 10:90 followed by CH₂Cl₂:EtOAc from 100:0 to 10:90, and EtOAc:MeOH from 100:0 to 50:50) to afford 206 fractions (30 mL each). The eluted fractions were evaluated and pooled, according to TLC analysis, to afford 16 fractions (F-1 to F-16). Fraction F-4 (352.0 mg) from *n*-hexane:CH₂Cl₂ 20:80 and 100% CH₂Cl₂ was further fractionated by column chromatography on silica gel that was treated with 10% NaHCO₃ solution, as described for the initial column chromatography yielding 33 fractions. These were grouped according to TLC analysis, into 9 fractions (F-4.1 to F-4.9). Fraction F-4.3 (150.0 mg) was purified by preparative TLC, eluted with 100% acetone, to give **5** (66.2 mg). Fraction F-5 (395.5 mg), from 100% CH₂Cl₂ and CH₂Cl₂:AcOEt 90:10, was fractionated as described for fraction F-4 to afford 9 fractions (F-5.1 to

F-5.9). Fraction F-5.2 (100 mg) furnished **5** (56.7 mg) after preparative TLC as described for F-4.3. Fraction F-5.3 (80.4 mg) was purified by preparative TLC, eluted with petroleum ether:acetone (70:30, two elutions), to yield **2** (6.5 mg), **3** (6.3 mg) and **4** (7.5 mg). Fraction F-5.5 (132.0 mg) was purified by preparative TLC, eluted with petroleum ether:acetone (60:40, three elutions), yielding **6** (5.0 mg), **7** (15.0 mg), **8** (1.0 mg) and **9** (1.1 mg). Fraction F-5.7 (24.8 mg) was purified by preparative TLC, eluted with petroleum ether:acetone (70:30, three elutions), affording **1** (10.6 mg). Fraction F-10 (219.9 mg), from AcOEt:CH₃OH 90:10, was fractionated as described for fraction F-4 to afford 36 fractions that were pooled into 8 fractions (F-10.1 to F-10.8), according to TLC analysis. Fraction F-10.2 yielded **10** (14.0 mg). Fraction F-10.7 (80.0 mg) was washed with CH₂Cl₂ and recrystallized in a mixture of CH₂Cl₂:MeOH (3:1) to give **11** (45.2 mg). Fraction F-11 (520.7 mg), from AcOEt:CH₃OH 80:20, was also washed with CH₂Cl₂ and recrystallized in a mixture of CH₂Cl₂:MeOH (3:1) furnishing **11** (357.0 mg).

13-Hydroxy-discretinine (1): yellowish amorphous powder; $[\alpha]_D^{25} -169.95^\circ$ (c 0.2, CHCl₃); UV (MeOH) λ_{\max}/nm (log ϵ) 206 (4.41), 226 (4.03), 282 (3.64), 336 (3.30); IR (KBr) $\nu_{\max}/\text{cm}^{-1}$ 3509, 3329, 2975, 2924, 2852, 2751, 1608, 1529, 1497, 1461, 1428, 1394, 1342, 1318, 1282, 1250, 1226, 1203, 1142, 1083, 1030, 965, 895, 865, 816, 792, 767, 665, 536; CD $\Delta\epsilon$ MeOH (λ/nm) +12.3 (229), -96.8 (242), +13.6 (276); ¹H and ¹³C NMR data see Table 1; HRESIMS m/z 358.1653 (calcd. for C₂₀H₂₃NO₅ + H⁺, 358.1654).

13-Hydroxy-2,3,9,10-tetramethoxyprotoberberine (2): yellowish amorphous powder; $[\alpha]_D^{25} -234.74^\circ$ (c 0.095, CHCl₃); UV (MeOH) λ_{\max}/nm (log ϵ) 204 (4.20), 226 (3.71), 280 (3.20), 347 (2.76); IR (KBr) $\nu_{\max}/\text{cm}^{-1}$ 3422, 2997, 2937, 2920, 2836, 1609, 1518, 1496, 1460, 1360, 1280, 1256, 1233, 1213, 1140, 1105, 1074, 1037, 1023, 1007, 976, 861, 820, 791, 752, 710, 663, 535, 428; CD $\Delta\epsilon$ MeOH (λ/nm) +6.8 (227), -25.3 (244), +7.3 (274); ¹H and ¹³C NMR data see Table 1; HRESIMS m/z 372.1808 (calcd. for C₂₁H₂₅NO₅ + H⁺, 372.1810).

6,6a-Dehydroguatterriopsiscine (3): white amorphous powder; $[\alpha]_D^{25} -198.46^\circ$ (c 0.325, CHCl₃); UV (MeOH) λ_{\max}/nm (log ϵ) 204 (4.04), 218 (3.86), 252 (4.00), 260 (4.09), 288 (3.63), 332 (3.12); IR (KBr) $\nu_{\max}/\text{cm}^{-1}$ 3188, 2991, 2967, 2930, 2906, 2860, 2829, 1629, 1575, 1490, 1473, 1444, 1413, 1381, 1344, 1323, 1282, 1205, 1140, 1094, 1081, 1038, 1008, 970, 953, 888, 824, 757, 729, 638, 596, 544; CD $\Delta\epsilon$ MeOH (λ/nm) -200.1 (313);

Table 1. NMR data (400 MHz, CDCl₃) for tetrahydroprotoberberine alkaloids **1** and **2**

Position	1				2			
	δ_c mult. ^a	δ_H mult. (J / Hz) ^a	HMBC ^b	NOE	δ_c mult. ^a	δ_H mult. (J / Hz) ^a	HMBC ^b	
1	107.6, CH	6.75 s	3, 4a, 13a and 13b	H ₃ CO-2 and H-13	108.3, CH	6.78 s	3, 4a, 13a and 13b	
2	145.5, qC				147.8, qC			
3	144.2, qC				147.6, qC			
4	114.3, CH	6.67 s	2, 5 and 13b	H-5 _{Pseudoeq}	111.4, CH	6.63 s	2, 5 and 13b	
4a	129.1, qC				128.3, qC			
5 _{Pseudoax}	28.8, CH ₂	3.07 ddd (15.7; 11.9; 5.0)		H-5 _{Pseudoeq} , H-6 _{Pseudoax} and H-6 _{Pseudoeq}	29.1, CH ₂	3.13 m	4a and 6	
5 _{Pseudoeq}		2.61 ddd (15.7; 2.9; 1.4)		H-5 _{Pseudoax} , H-6 _{Pseudoax} and H-6 _{Pseudoeq}		2.64 m	4, 4a and 13b	
6 _{Pseudoax}	51.0, CH ₂	2.70 ddd (11.9; 10.8; 2.9)	13a	H-6 _{Pseudoeq} , H-5 _{Pseudoax} and H-5 _{Pseudoeq}	51.0, CH ₂	2.73 m	4a and 13a	
6 _{Pseudoeq}		3.18 ddd (10.8; 5.0; 1.4)	4a, 5 and 13a	H-8 _{Pseudoeq} , H-6 _{Pseudoax} and H-5 _{Pseudoeq}		3.20 m	4a, 5, 8 and 13a	
8 _{Pseudoax}	53.9, CH ₂	3.54 d (16.0)	6, 8a, 9 and 12	H-8 _{Pseudoeq}	53.9, CH ₂	3.56 d (16.0)	6, 8a, 9, 12a and 13a	
8 _{Pseudoeq}		4.21 d (16.0)	8a, 9, 12a and 13a	H-8 _{Pseudoax}		4.22 d (16.0)	6, 8a, 9, 12a and 13a	
8a	128.7, qC				128.7, qC			
9	144.6, qC				144.7, qC			
10	151.7, qC				151.7, qC			
11	111.1, CH	6.88 d (8.3)	9 and 12a	H ₃ CO-10 and H-12	111.1, CH	6.88 d (8.4)	9 and 12a	
12	125.3, CH	7.17 d (8.3)	8a, 10 and 13	H-11 and H-13	125.3, CH	7.18 d (8.4)	8a, 10, 11 and 13	
12a	130.9, qC				131.0, qC			
13	69.9, CH	4.80 br s	8a, 12 and 13b	H-1, H-12 and H-13a	69.9, CH	4.82 br s	8a, 12 and 12a	
13a	64.4, CH	3.68 br s	8 and 13b	H-1, H-8 _{Pseudoax} and H-13	64.3, CH	3.70 br s	1, 4a, 8 and 13b	
13b	125.4, qC				126.0, qC			
H ₃ CO-2	55.9, CH ₃	3.89 s	2	1	56.0, CH ₃	3.90 s	2	
H ₃ CO-3					55.8, CH ₃	3.87 s	3	
H ₃ CO-9	60.1, CH ₃	3.86 s	9	H ₃ CO-10	60.1, CH ₃	3.86 s	9	
H ₃ CO-10	55.8, CH ₃	3.87 s	10	H ₃ CO-9 and 11	55.8, CH ₃	3.88 s	10	

^aThe experiments were acquired at 293 K with TMS as internal reference at 0.00 ppm; ^blong-range ¹H-¹³C correlations (HMBC), optimized for 8 Hz, are from the stated hydrogens to the indicated carbon.

¹H and ¹³C NMR data see Table 2; HRESIMS *m/z* 354.1705 (calcd. for C₂₁H₂₃NO₄ + H⁺, 354.1705).

9-Dehydroxy-1-methoxy-dihydroguattouregidine (**4**): brown amorphous powder; [α]_D²⁵ -25.80° (*c* 0.155, CHCl₃); UV (MeOH) λ_{max} /nm (log ϵ) 211 (4.35), 240 (3.96), 262 (3.95), 277 (4.01); IR (KBr) ν_{max} /cm⁻¹ 3295, 2935, 2848, 1685, 1581, 1457, 1414, 1338, 1288, 1199, 1167, 1121, 1083, 1030, 997, 945, 826, 758, 651, 503; ¹H and ¹³C NMR data see Table 2; HRESIMS *m/z* 342.1700 (calcd. for C₂₀H₂₃NO₄ + H⁺, 342.1705).

Cell culture and *in vitro* cytotoxic assay

Human tumor cell lines U251 (glioma), UACC-62 (melanoma), MCF-7 (breast), NCI-H460 (lung, non-small cells), PC-3 (prostate) and K562 (leukaemia) were kindly provided by the Frederick Cancer Research & Development Center, National Cancer Institute (NCI, USA). The human keratinocyte (HaCaT) cell line was donated by Dr. Ricardo Della Coletta from Piracicaba Dental School, Universidade Estadual de Campinas (Brazil). Stock cultures were grown in medium containing 5 mL RPMI 1640

(GIBCOR BRL) supplemented with 5% fetal bovine serum. Penicillin:streptomycin (1000 μ g mL⁻¹:1000 UI mL⁻¹, 1 mL L⁻¹) was added to experimental cultures. Cells in 96 well plates (100.0 μ L cells well⁻¹) were exposed to sample concentrations of 0.25, 2.5, 25 and 250 μ g mL⁻¹ in DMSO/RPMI at 37 °C and 5% CO₂ in air for 48 h. The final dimethyl sulfoxide (DMSO) concentration did not affect the cell viability. Subsequently, cells were fixed with 50% trichloroacetic acid, and cell proliferation was determined by spectrophotometric quantification (540 nm) of the cellular protein content using the sulforhodamine B assay. Absorbance was measured at the beginning of the incubation and 48 h post-incubation for compound-free (T1) and tested (T) cells.¹⁵ Cell proliferation was determined according to the equation 100 [(T - T0)/(T1 - T0)], for T0 < T ≤ T1, and 100 [(T - T0)/T0], for T ≤ T0. Using the concentration-response curve for each cell line, GI₅₀ values (concentration that causes 50% growth inhibition) were determined through a non-linear regression analysis (Table 3). Samples were regarded as inactive (mean > 1.5), weakly (1.1 < mean < 1.5), moderately (0 < mean < 1.1) or potently (mean < 0) active based on the NCI criteria for the mean of log GI₅₀.¹⁶

Table 2. NMR data (400 MHz, CDCl₃) for aporphine alkaloids **3** and **4**

Position	3				4			
	δ_c mult. ^a	δ_H mult. (J / Hz) ^a	HMBC ^b	NOE	δ_c mult. ^a	δ_H mult. (J / Hz) ^a	HMBC ^b	NOE
1	152.0, qC				149.8, qC			
1a	122.9, qC				121.5, qC			
2	149.4, qC				145.6, qC			
3	149.9, qC				150.9, qC			
3a	126.2, qC				125.4, qC			
3b	118.5, qC				128.0, qC			
4 _{Pseudoax}	59.4, CH	4.98 dd (4.2; 2.4)	3, 3a and 3b	H ₃ CO-3 and	23.5, CH ₂	2.72 ddd (17.1; 12.0; 6.2)	3a and 3b	
4 _{Pseudoeq}				H-5 _{Pseudoax/Pseudoeq}		2.82 ddd (17.1; 4.5; 1.4)	3, 3a, 3b and 5	
5 _{Pseudoax}	54.8, CH ₂	3.48 dd (16.6; 4.2)	3a, 3b, 6a and 7		42.4, CH ₂	2.98 ddd (12.3; 12.0; 4.5)	3a and 6a	
5 _{Pseudoeq}		4.40 dd (16.6; 2.4)	3a, 4, and 6a			3.49 ddd (12.3; 6.2; 1.4)	3a, 4 and 6a	
6a	170.4, qC				61.3, CH	3.77 s	1a, 3a, 3b and 7a	H ₃ C-7 _{Pseudoax}
7	42.7, qC				70.7, qC			
7a	143.7, qC				138.9, qC			
8	124.6, CH	7.54 m	7, 10 and 11a		124.2, CH	7.60 ddd (7.8; 1.3; 0.4)	7, 10 and 11a	
9	128.2, CH	7.30 m	7a, 8, 11 and 11a		127.4, CH	7.30 ddd (7.8; 7.4; 1.4)	7a and 11	
10	126.7, CH	7.30 m	8, 11 and 11a		128.5, CH	7.38 ddd (7.8; 7.4; 1.3)	8 and 11a	
11	127.8, CH	8.46 m	1a, 7a and 9	H ₃ CO-1 and 10	128.4, CH	8.38 ddd (7.8; 1.4; 0.4)	1a, 7a and 9	
11a	129.4, qC				130.6, qC			
H ₃ CO-1	60.9, CH ₃	3.84 s	1	H ₃ CO-2 and 11	60.7, CH ₃	3.73 s	1	11
H ₃ CO-2	61.1, CH ₃	4.04 s	2		60.9, CH ₃	3.96 s	2	
H ₃ CO-3	61.8, CH ₃	4.03 s	3		60.4, CH ₃	3.92 s	3	
H ₃ C-7 _{Pseudoax}	22.6, CH ₃	1.71 s	6a, 7a, 8 and H ₃ C-7 _{Pseudoeq}		22.1, CH ₃	1.79 s	6a, 7, 7a and 8	H-6a and H-8
H ₃ C-7 _{Pseudoeq}	32.0, CH ₃	1.38 s	6a, 7a, 8 and H ₃ C-7 _{Pseudoax}					

^aThe experiments were obtained at 293 K with TMS as internal reference at 0.00 ppm; ^blong-range ¹H-¹³C correlations (HMBC), optimized for 8 Hz, are from the stated hydrogens to the indicated carbon.

Table 3. *In vitro* cytotoxic activity for extracts and alkaloids of *G. friesiana*

Extract/Fraction	GI ₅₀ / (μg mL ⁻¹) ^a							Mean log GI ₅₀ ^b	HaCat
	U251	UACC-62	MCF-7	NCI-H460	PC-3	K-562			
MeOH extract	57.3	30.0	35.9	59.2	40.4	40.1	1.6 I	35.1	
CH ₂ Cl ₂ alkaloid fraction	53.0	32.2	26.5	28.6	27.8	53.3	1.5 I	26.8	
CH ₂ Cl ₂ neutral fraction	25.9	27.5	25	27.7	25	22.4	1.4 W	24.8	
Alkaloid	GI ₅₀ / (μmol L ⁻¹) ^b								
1	174.4	80.1	73.4	78.7	80.4	154.6	2.0 I	76.2	
2	> 673.5	> 673.5	673.5	> 673.5	> 673.5	673.5	2.8 I	673.5	
3	409.2	282.6	107.6	327.9	150.9	502.6	2.4 I	183.2	
4	725.2	732.8	32.8	628.1	300.2	593.3	2.5 I	610.8	
5	> 703.9	> 703.9	703.9	> 703.9	703.9	> 703.9	2.8 I	> 703.9	
10	118.9	83.7	73.1	370.3	220.0	138.2	2.2 I	77.2	
11	16.2	94.3	10.5	190.5	117.8	113.9	1.8 I	122.1	
Doxorubicin ^c	0.043	0.067	0.043	0.043	0.33	0.11	-1.1 P	0.043	

^aGI₅₀ (growth inhibition 50): concentration that causes 50% growth inhibition; ^bmean log GI₅₀: average activity of tested samples. NCI criteria: W, weak activity: log GI₅₀ > 1.10-1.5; M, moderate activity: log GI₅₀ > 0-1.10; P, potent activity: log GI₅₀ < 0.¹⁶ ^cReference drug (positive control). Human cancer cell lines: U251 (glioma, CNS), UACC-62 (melanoma), MCF-7 (breast), NCI-H460 (lung non-small cells), PC-3 (prostate) and K562 (leukaemia). Human non-cancer cell line: HaCat (keratinocytes).

Results and Discussion

Compound **1** was isolated as a yellowish amorphous powder, optically active, [α]_D²⁵ -169.95° (*c* 0.2, CHCl₃),

with the molecular formula C₂₀H₂₃NO₅, as determined by HRESIMS (observed *m/z* 358.1653 [M + H]⁺) and NMR data. The IR spectrum showed absorption bands at 3329 and 1608 cm⁻¹, characteristic of hydroxyl groups and aromatic

ring systems, respectively. The UV spectrum showed maximum absorptions at 206, 226, 282 and 336 nm. The ^1H and $^{13}\text{C}\{^1\text{H}\}$ NMR spectra indicated the presence of a tetrahydroprotoberberine skeleton. The ^1H NMR spectrum showed three methoxy signals at δ 3.86, 3.87 and 3.89 (s, 3H each) and four aromatic hydrogens, two at δ 6.75 and 6.67 (s, 1H each), and two at δ 7.17 and 6.88 (d, 1H each, J 8.3 Hz), suggesting a 2,3,9,10-tetraoxygenated tetrahydroprotoberberine alkaloid structure (Figure 1), such as discretinine.⁸ The main difference between the ^1H NMR of discretinine and that of **1** was the signal for a carbinolic hydrogen at δ 4.80 (s, 1H), attributed to H-13. The $^{13}\text{C}\{^1\text{H}\}$ NMR spectrum showed 20 carbons, 12 aromatic carbons between δ 151.8 and 107.6, three methoxy carbons at δ 60.1, 55.9 and 55.8, three methylenes at δ 53.9, 51.0 and 28.8, and two methines at δ 69.9 and 64.4, consistent with the structure **1**. The structure of compound **1** was fully established by HSQC, HMBC and 1D NOE NMR experiments (Table 1). The assignment of H-13 was made with the aid of an HMBC correlation map that showed correlations of the carbinolic hydrogen at δ 4.80 (H-13) with the carbons at δ 125.3, (C-12), 128.7 (C-8a) and 125.4 (C-13b) (Table 1). In the same way, the hydroxyl group at C-3 was established based on the long-range ^1H - ^{13}C correlation between H-1 (δ 6.75) and C-3 at δ 144.2, which showed no correlation with any of the three remaining methoxy groups (Table 1). Therefore, compound **1** was established as a novel tetrahydroprotoberberine alkaloid, named 13-hydroxy-discretinine. The absolute configurations of the stereocenters (C-13a and C-13) of the 13-hydroxyprotoberberines are well known from the literature.¹⁷⁻²⁰ Two 13-hydroxyprotoberberines, ophiocarpine and epiophiocarpine, for which the absolute configurations were determined, were used as models (Figure 2). The absolute configuration of C-13a of these alkaloids was established based on their optical rotations and can either have α or β orientation.¹⁸ The absolute configurations of tetrahydroprotoberberine alkaloids that are not substituted at C-13 were determined by Corrodi and Hardegger.²¹ A negative rotation or a negative Cotton effect was shown for the α -orientation.²¹ Additionally, Ohta *et al.*¹⁷ showed that the introduction of an additional asymmetric center at C-13 does not appear to affect the signal rotation when the group introduced is a hydroxyl. Both (–)-ophiocarpine and (–)-epiophiocarpine, with $[\alpha]_{\text{D}} -283^\circ$ (c 1.0, CHCl_3) and $[\alpha]_{\text{D}} -282^\circ$ (c 1.0, CHCl_3), respectively, having the absolute configuration displayed (Figure 2), show negative rotatory dispersion curves and negative optical rotation. This behavior is similar to that of (–)-canadine, which exhibits $[\alpha]_{\text{D}} -300^\circ$ (CHCl_3).¹⁷ The configuration of the hydroxyl group at C-13 in both

(–)-ophiocarpine and (–)-epiophiocarpine was established by infrared studies and pKa values, as well as through NMR studies as described by Ohta *et al.*¹⁷ This hydroxyl group has an axial configuration in (–)-ophiocarpine and an equatorial configuration in (–)-epiophiocarpine (Figure 2). Thus, the negative optical rotation of **1** is consistent with a C-13a *R*-configuration or an α -orientation. These findings were confirmed by the circular dichroism curve that showed a negative Cotton effect at 242 nm (-96.8). Having established the absolute configuration of C-13a, the absolute configuration of C-13 was determined through 1D NOE experiments that showed a *cis* relationship between H-13 and H-13a. In this experiment, the selective irradiation of the resonance frequency of H-13a at δ 3.68 caused a NOE enhancement of the signals at δ 6.75 (H-1), 4.80 (H-13), 3.54 (H-8 pseudoaxial) and 2.70 (H-6 pseudoaxial) (Table 1). Moreover, selective irradiation of the resonance frequency of H-13 at δ 4.80 showed NOE intensification of the signals at δ 3.68 (H-13a), 7.17 (H-12) and 6.75 (H-1). Thus, the absolute configuration of C-13 was established as *R* (Figure 1).

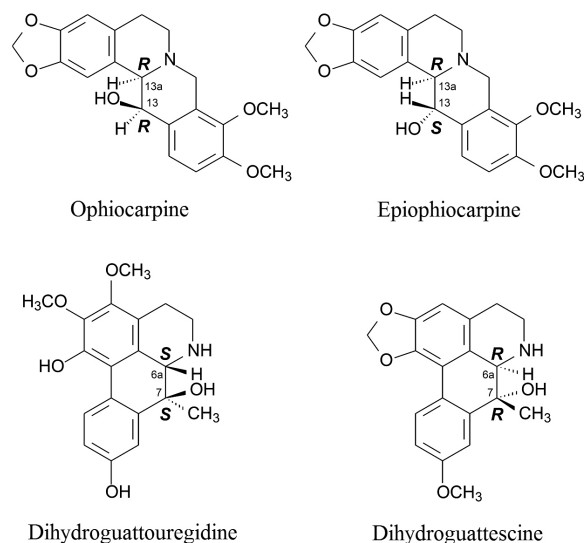


Figure 2. Structures of 13-hydroxytetrahydroprotoberberine alkaloids, (–)-ophiocarpine and (–)-epiophiocarpine, and 7-hydroxy-7-methylaporphine alkaloids, (–)-dihydroguattouregidine and (+)-dihydroguattescine, showing their absolute configurations.

Compound **2** was isolated as a yellowish amorphous powder, optically active $[\alpha]_{\text{D}}^{25} -234.74^\circ$ (c 0.095, CHCl_3), with the molecular formula $\text{C}_{21}\text{H}_{25}\text{NO}_5$, as determined by HRESIMS (observed m/z 372.1808 $[\text{M} + \text{H}]^+$) and NMR data. Its IR, UV and ^1H and $^{13}\text{C}\{^1\text{H}\}$ NMR spectra were very similar to those of **1**. The main difference between them was an additional signal for a methoxy group in the ^1H NMR spectra of **2** at δ 3.87 (s, 3H, H_3CO -3) that showed correlation with the carbon at δ

55.8 in the HSQC correlation map. The location of this additional methoxy group at C-3 was established with the aid of the HMBC correlation map, in which both hydrogens from the methoxy group at δ 3.87 and H-1 at δ 6.78 showed correlation with the same carbon at 147.6 (C-3) (Table 1). Therefore, compound **2** was identified as the tetrahydroprotoberberine alkaloid 13-hydroxy-2,3,9,10-tetramethoxyprotoberberine. This compound is known from a synthetic origin,²² although its absolute configuration at C-13a and C-13 was not previously established. The isolation of this compound as a natural product is here described for the first time. As observed for **1**, the negative optical rotation of **2** was consistent with a C-13a *R*-configuration, thus having an α -orientation.¹⁶ The same findings were observed on the circular dichroism curve that showed a negative Cotton effect at 244 nm (-25.3). The absolute configuration of C-13 was also established as *R*, according to 1D NOE experiments.

Compound **3** was isolated as a white amorphous powder, optically active [α]_D²⁵ -198.46° (*c* 0.325, CHCl₃), with the molecular formula C₂₁H₂₃NO₄, as determined by HRESIMS (observed *m/z* 354.1705 [M + H]⁺) and NMR data. Its IR, UV, ¹H and ¹³C{¹H} NMR spectra were very similar to those reported for the alkaloid guatterioipsiscine (**5**).⁸ The main difference between them was the signal corresponding to an imine group (C=N) carbon at δ 170.4, that was absent in **5**, indicating a double bond between C-6a and N-6 in **3** (Figure 1).⁸ The assignment of the imine group was made through the ¹H-¹³C long-range correlation map due to the correlation between hydrogens at δ 4.40 (H-5 pseudoaxial) and 3.48 (H-5 pseudoequatorial), as well as the correlations of methyl hydrogens at δ 1.71 (H₃C-7 pseudoaxial) and 1.38 (H₃C-7 pseudoequatorial) with the carbon at δ 170.4 (C-6a) (Table 2). The structure of **3** was fully supported by the HSQC, HMBC and 1D NOE NMR experiments (Table 2). Therefore, compound **3** was established as a novel 7,7-dimethylaporphine alkaloid, named 6,6a-dehydroguatterioipsiscine. The relative stereochemistry of the chiral center at C-4 was established by 1D NOE experiments and comparison with the NMR data of guatterioipsiscine (**5**).⁸ Selective irradiation of the resonance frequency of the H-4 at δ 4.98 caused a NOE intensification of the signals at δ 4.03 (H₃CO-3) as well as of the signals at δ 4.40 (H-5 pseudoaxial) and 3.48 (H-5 pseudoequatorial) (Table 1). These relationships are in full accordance with the substitution pattern of the aporphine alkaloids.

Compound **4** was isolated as a brown amorphous powder, optically active [α]_D²⁵ -25.80° (*c* 0.155, CHCl₃), with the molecular formula C₂₀H₂₃NO₄, as determined by HRESIMS (observed *m/z* 342.1700 [M + H]⁺) and

NMR data. Its IR, UV, and ¹H and ¹³C{¹H} NMR spectra were very similar to those reported for the alkaloid dihydroguattouregidine (Figure 2).²³ The main difference between them was the absence of the hydroxy group at C-1, which was replaced in **4** by a methoxy group according to the additional signal at δ 3.73 in the ¹H NMR spectrum. These hydrogens showed correlation with the carbon at δ 60.7 in the HSQC correlation map (Table 2). The presence of the methoxy group at C-1 was supported by 1D NOE experiments, in which selective irradiation of the resonance frequency of the methoxy group at δ 3.73 (H₃CO-1) caused NOE enhancement of the signal at δ 8.38 (H-11) (Table 2). Moreover, the ¹H NMR spectrum of **4** revealed a spin system consisting of four aromatic hydrogens (Table 2). The complete structure elucidation and unambiguous ¹H and ¹³C NMR chemical shift assignments of **4** were supported by HSQC, HMBC and 1D NOE NMR experiments (Table 2). Therefore, compound **4** was established as a novel 7,7-dimethylaporphine alkaloid, named 9-dehydroxy-1-methoxy-dihydroguattouregidine. As observed for tetrahydroprotoberberine alkaloids, the absolute configuration of the chiral center C-6a is well known from the literature and could be established by analysis of its optical rotation.²³⁻²⁵ Two alkaloids, dihydroguattouregidine and dihydroguattescine, for which the absolute configurations have been determined, were used as models in this assignment (Figure 2). In (–)-dihydroguattouregidine, the circular dichroism spectrum showed a negative Cotton effect at 233 nm and [α]_D -12.0° , indicating that the hydrogen at C-6a has a β -orientation, and consequently, the configuration of C-6a is *S*.^{23,24} However, in (+)-dihydroguattescine the circular dichroism spectrum showed a positive Cotton effect at 235 nm and [α]_D $+49.0^\circ$, indicating that the hydrogen at C-6a has an α -orientation and, consequently, the configuration of C-6a is *R*.^{24,25} The optical rotation [α]_D²⁵ -25.80° of alkaloid **4** reveals that the hydrogen at C-6a has a β -orientation, and thus, the configuration of C-6a is *S*, as observed for (–)-dihydroguattouregidine (Figure 2). Having established the absolute configuration of C-6a, the absolute configuration of C-7 was determined by 1D NOE NMR experiments. In these experiments, the selective irradiation of the resonance frequency of H-6a at δ 3.77 caused the NOE enhancement of the signal at δ 1.79 (H₃C-7 pseudoaxial). Moreover, the selective irradiation of the resonance frequency of the methyl hydrogens at δ 1.79 (H₃C-7 pseudoaxial) showed NOE intensification of the signals at δ 7.60 (H-8) and 3.77 (H-6a). Thus, the absolute configuration of C-7 was established as *R*.

Compounds **5-11** were identified by comparison of their spectrometric data with those described in the literature for

guatterioipiscine (**5**),⁸ lysicamine (**6**),^{4,26} liriodenine (**7**),^{8,27} atherospermidine (**8**),²⁷ lanuginosine (**9**),²⁸ 7,8-dihydro-8-hydroxypalmatine (**10**)²⁹ and palmatine (**11**).²⁹

The methanolic extract, CH₂Cl₂ alkaloid and CH₂Cl₂ neutral fractions of *G. friesiana* leaves were then evaluated against several human cell lines in order to determine whether or not they exhibited any cytotoxic effects. All of the tested samples showed an unspecific weak cytostatic effect, according to the NCI criteria.¹⁶ Only the CH₂Cl₂ neutral fraction had weak cytotoxic activity, while the MeOH extract and CH₂Cl₂ alkaloid fraction were considered to be inactive (Table 3).

The cytotoxic activity of the major alkaloids, except **6-9**, was also evaluated against tumor cell lines. The cytotoxic profile of alkaloids **6** and **7** was recently described by our research group,⁴ while alkaloids **8** and **9** were not investigated due to the low yields obtained. Considering the average activity of these compounds in the context of NCI criteria,¹⁶ all of the alkaloids evaluated (**1-5**, **10-11**) were inactive. On the other hand, it is interesting to notice that the alkaloid palmatine (**11**) showed selective cytotoxic activity against MCF-7 (breast, GI₅₀ = 10.5 μmol L⁻¹) and U251 (glioma, GI₅₀ = 16.2 μmol L⁻¹) cell lines. This selectivity to U251 and MCF-7 cell lines could be attributed to the quaternary nitrogen in the structure of **11**. Alkaloid **10**, which has a very similar structure to **11** except for the absence of the quaternary nitrogen, shows higher GI₅₀ values against MCF-7 (breast, GI₅₀ = 73.1 μmol L⁻¹) and U251 (glioma, GI₅₀ = 118.9 μmol L⁻¹) cell lines. Moreover, palmatine (**11**) was almost eleven times less toxic against a normal cell line (HaCat, human keratinocytes), with a GI₅₀ value of 122.1 μmol L⁻¹. This activity is reduced compared to that observed for the breast tumor cell line, suggesting selective activity against tumor cell lines (Table 3).

Conclusions

The chemical investigation of the leaves of *Guatteria friesiana* resulted in the isolation and characterization of three new isoquinoline alkaloids, 13-hydroxy-discretinine (**1**), 6,6a-dehydroguatterioipiscine (**3**), and 9-dehydroxy-1-methoxy-dihydroguattouregidine (**4**), along with eight other known alkaloids (**2**, **5-11**). However, alkaloid 13-hydroxy-2,3,9,10-tetramethoxyprotoberberine (**2**) from a natural source is reported for the first time. The presence of aporphine and tetrahydroprotoberberine alkaloids in the leaves of *G. friesiana* is consistent with previous phytochemical and chemotaxonomic studies of the family Annonaceae. All of the alkaloids evaluated herein were found to be inactive

against tumor cell lines when their average activities were judged against of NCI criteria. However, palmatine (**11**) showed a cytostatic effect against MCF-7 (breast) and U251 (glioma) human tumor cell lines and very low cytotoxicity toward a normal cell line (HaCat, human keratinocytes), suggesting selective cytotoxic activity.

Supplementary Information

Supplementary information containing 1D and 2D NMR, and MS data for alkaloids **1-4** is available free of charge at <http://jbcbs.s bq.org.br> as a PDF file.

Acknowledgments

The authors are grateful to Prof. Dr. Norberto P. Lopes and José Carlos Tomaz from the Faculdade de Ciências Farmacêuticas de Ribeirão Preto (USP, Brazil), for HRESIMS analysis, Prof. Dr. Fábio Cesar Gozzo from the Universidade Estadual de Campinas (Unicamp, Brazil), for circular dichroism analyses, Prof. Dr. Antonio C. Webber from the Universidade Federal do Amazonas (UFAM, Brazil) for the botanical identification, as well as to CAPES, CNPq, FINEP, UFPR and the Fundação Araucária for financial support and research fellowships.

References

1. Chatrou, L. W.; Pirie, M. D.; Erkens, R. H. J.; Couvreur, T. L. P.; Neubig, K. M.; Abbott, J. R.; Mols, J. B.; Maas, J. W.; Saunders, R. M. K.; Chase, M. W.; *Bot. J. Linn. Soc.* **2012**, *169*, 5.
2. Erkens, R. H. J.; Maas, P. J. M.; *Rodriguésia* **2008**, *59*, 401.
3. Corrêa, M. P.; *Dicionário das Plantas Úteis do Brasil e das Exóticas Cultivadas*; IBDF: Rio de Janeiro, Brasil, 1984.
4. Costa, E. V.; Marques, F. A.; Pinheiro, M. L. B.; Braga, R. M.; Delarmelina, C.; Duarte, M.C.T.; Ruiz, A. L. T. G.; Carvalho, J. E.; Maia, B. H. L. N. S.; *J. Braz. Chem. Soc.* **2011**, *22*, 1111.
5. Palazzo, M. C.; Wright, H. L.; Agius, B. R.; Wright, B. S.; Moriarity, D. M.; Haber, W. A.; Setzer, W. N.; *Rec. Nat. Prod.* **2009**, *3*, 153.
6. Brito, A. C. S.; Oliveira, A. C.; Henriques, R. M.; Cardoso, G. M. B.; Bomfim, D. S.; Carvalho, A. A.; Moraes, M. O.; Pessoa, C.; Pinheiro, M. L. B.; Costa, E. V.; Bezerra, D. P.; *Planta Med.* **2012**, *78*, 409.
7. Costa, E. V.; Pinheiro, M. L. B.; Barison, A.; Campos, F. R.; Salvador, M. J.; Maia, B. H. L. N. S.; Cabral, E. C.; Eberlin, M. N.; *J. Nat. Prod.* **2010**, *73*, 1180.
8. Costa, E. V.; Marques, F. A.; Pinheiro, M. L. B.; Vaz, N. P.; Duarte, M. C. T.; Delarmelina, C.; Braga, R. M.; Maia, B. H. L. N. S.; *J. Nat. Prod.* **2009**, *72*, 1516.

9. Costa, E. V.; Teixeira, S. D.; Marques, F. A.; Duarte, M. C. T.; Delarmelina, C.; Pinheiro, M. L. B.; Trigo, J. R.; Maia, B. H. L. N. S.; *Phytochemistry* **2008**, *69*, 1895.
10. Zhang, Z.; ElSohly, H. N.; Jacob, M. R.; Pasco, D. S.; Walker, L. A.; Clark, A. M.; *J. Nat. Prod.* **2002**, *65*, 856.
11. Montenegro, H.; Gutiérrez, M.; Romero, L. I.; Ortega-Barría, E.; Capson, T. L.; Rios, L. C.; *Planta Med.* **2003**, *69*, 677.
12. Mahiou, V.; Roblot, F.; Fournet, A.; Hocquemiller, R.; *Phytochemistry* **2000**, *54*, 709.
13. Aciole, S. D. G.; Piccoli, C. F.; Duque, L. J. E.; Costa, E. V.; Navarro-Silva, M. A.; Marques, F. A.; Maia, B. H. L. N. S.; Pinheiro, M. L. B.; Rebelo, M. T.; *Rev. Colomb. Entomol.* **2011**, *37*, 262.
14. Costa, E. V.; Pinheiro, M. L. B.; Xavier, C. M.; Silva, J. R. A.; Amaral, A. C. F.; Souza, A. D. L.; Barison, A.; Campos, F. R.; Ferreira, A. G.; Machado, G. M. C.; Leon, L. L. P.; *J. Nat. Prod.* **2006**, *69*, 292.
15. Shoemaker, R. H.; *Nat. Rev. Cancer* **2006**, *6*, 813.
16. Fouche, G.; Cragg, G. M.; Pillay, P.; Kolesnikova, N.; Maharaj, V. J.; Senabe, J.; *J. Ethnopharmacol.* **2008**, *119*, 455.
17. Ohta, M.; Tani, H.; Morozumi, S.; *Chem. Pharm. Bull.* **1964**, *12*, 1072.
18. Jeffs, P. W.; *Experientia* **1965**, *21*, 690.
19. Snatzke, G.; Hrbek Jr., J.; Hruban, L.; Horeau, A.; Santavý, F.; *Tetrahedron* **1970**, *26*, 5013.
20. Iwasa, K.; Sugiura, M.; Takao, N.; *J. Org. Chem.* **1982**, *47*, 4275.
21. Corrodi, H.; Hardegger, E.; *Helv. Chim. Acta* **1956**, *39*, 889.
22. Govindachari, T. R.; Rajadurai, S.; Subramanian, M.; Viswanathan, N.; *J. Chem. Soc.* **1957**, 2943.
23. Leboeuf, M.; Cortes, D.; Hocquemiller, R.; Cavé, A.; *Planta Med.* **1983**, *48*, 234.
24. Ringdahl, B.; Chan, R. P. K.; Craig, J. C.; Cava, M. P.; Shamma, M.; *J. Nat. Prod.* **1981**, *44*, 80.
25. Hocquemiller, R.; Rasamizafy, S.; Cavé, A.; *J. Nat. Prod.* **1983**, *46*, 335.
26. Chang, F.-R.; Chen, C.-Y.; Hsieh, T.-J.; Cho, C.-P.; Wu, Y.-C.; *J. Chin. Chem. Soc.* **2000**, *47*, 913.
27. Costa, E. V.; Pinheiro, M. L. B.; Souza, A. D. L.; Barison, A.; Campos, F. R.; Valdez, R. H.; Ueda-Nakamura, T.; Dias Filho, B. P.; Nakamura, C. V.; *Molecules* **2011**, *16*, 9714.
28. Wirasathien, L.; Pengsuparp, T.; Moriyasu, M.; Kawanishi, K.; Suttisri R.; *Arch. Pharm. Res.* **2006**, *29*, 497.
29. Wafo, P.; Nyasse, B.; Fontaine, C.; *Phytochemistry* **1999**, *50*, 279.

Submitted: January 22, 2013

Published online: April 30, 2013

FAPESP has sponsored the publication of this article.

Aporphine and Tetrahydroprotoberberine Alkaloids from the Leaves of *Guatteria friesiana* (Annonaceae) and their Cytotoxic Activities

Emmanoel Vilaça Costa,^{*,a,b} Pedro Ernesto O. da Cruz,^a Maria Lúcia B. Pinheiro,^c
Francisco A. Marques,^b Ana Lúcia T. G. Ruiz,^d Gabriela M. Marchetti,^d
João Ernesto de Carvalho,^d Andersson Barison^b and Beatriz Helena L. N. S. Maia^b

^aDepartamento de Química, Universidade Federal de Sergipe,
Av. Marechal Rondon, s/n, Rosa Elze, 49100-000 São Cristóvão-SE, Brazil

^bDepartamento de Química, Universidade Federal do Paraná, Centro Politécnico,
Jardim das Américas, 81531-990 Curitiba-PR, Brazil

^cDepartamento de Química, Universidade Federal do Amazonas, Mini-Campus,
Av. General Rodrigo Otávio Jordão Ramos, 3000, Coroadó, 69077-000 Manaus-AM, Brazil

^dDivisão de Farmacologia e Toxicologia, Centro Pluridisciplinar de Pesquisas Químicas,
Biológicas e Agrícolas, Universidade Estadual de Campinas, 13083-970 Campinas-SP, Brazil

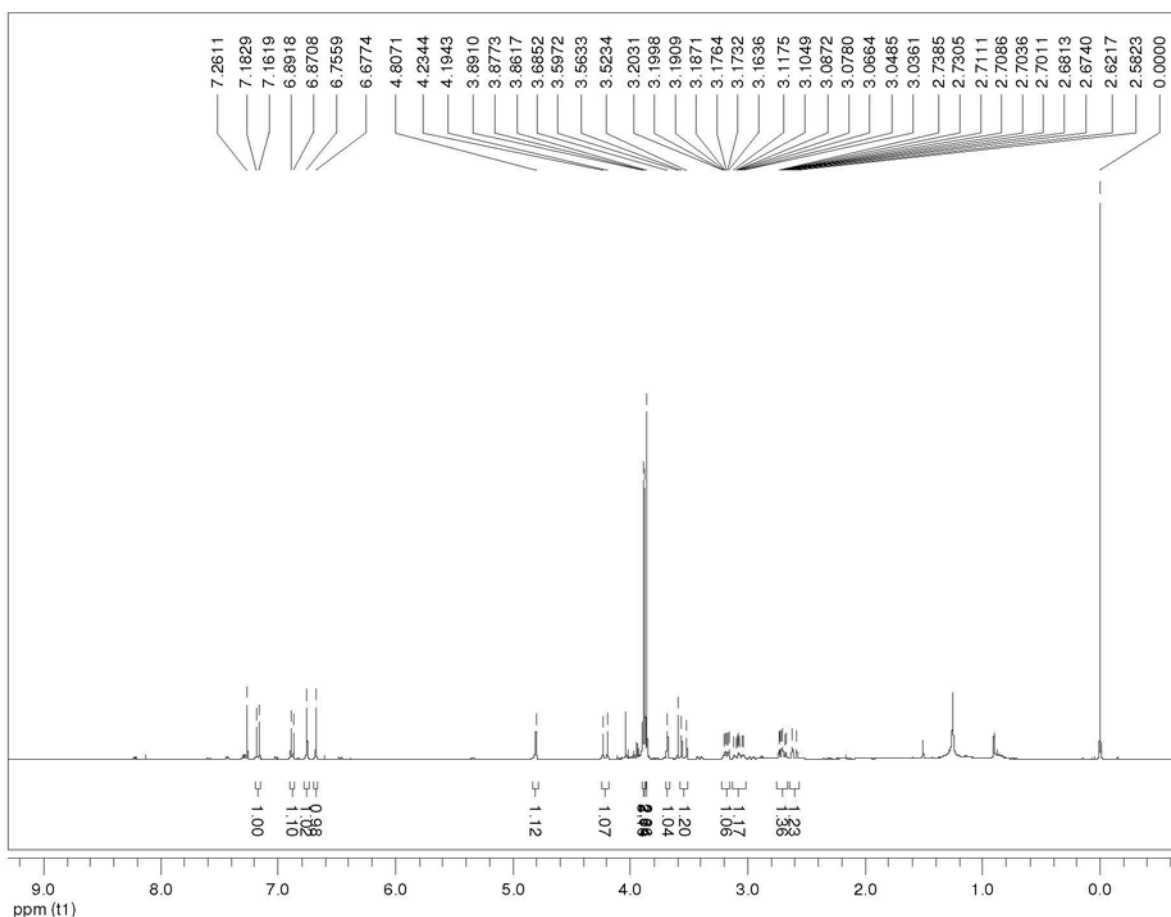


Figure S1. ¹H NMR spectrum of alkaloid **1** in CDCl₃ at 400 MHz.

*e-mail: emmanoelvc@gmail.com

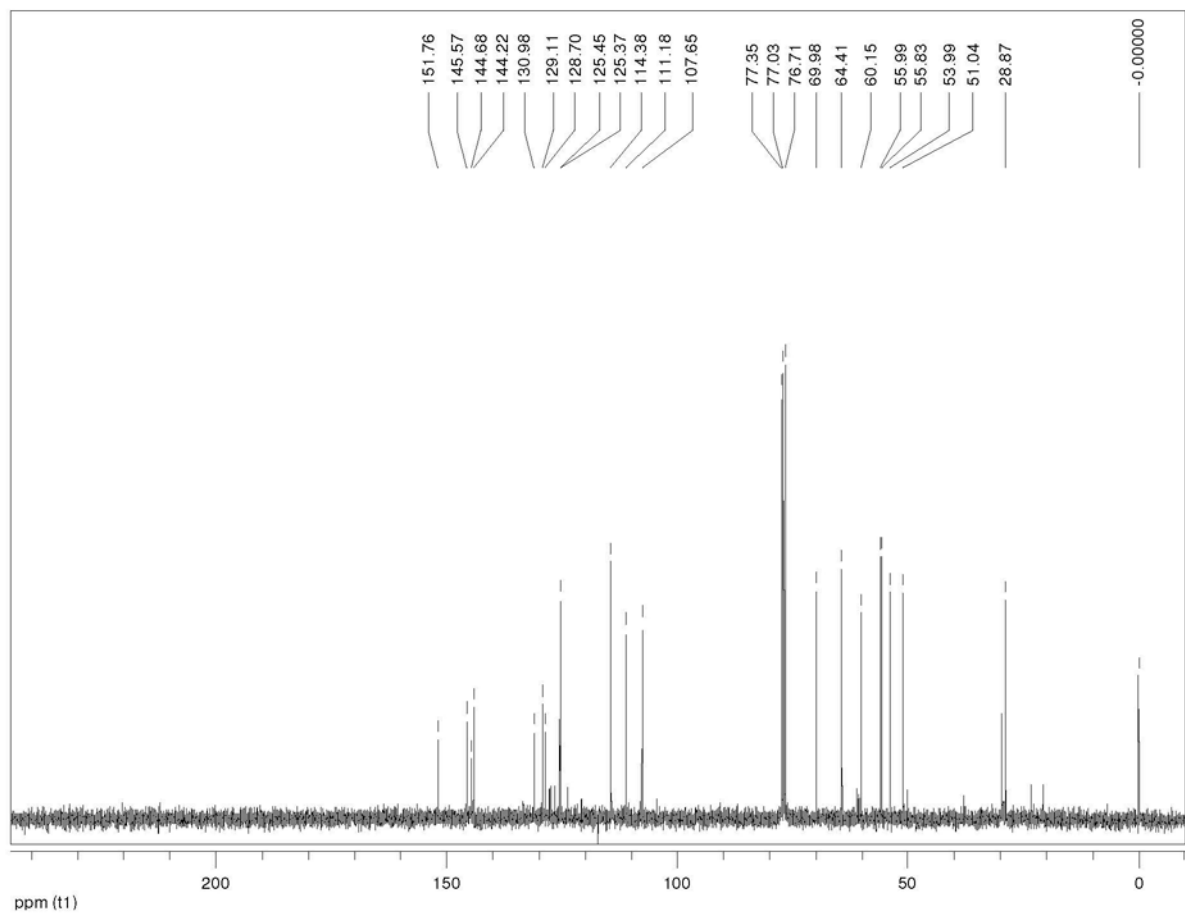


Figure S2. $^{13}\text{C}\{^1\text{H}\}$ NMR spectrum of alkaloid **1** in CDCl_3 at 100 MHz.

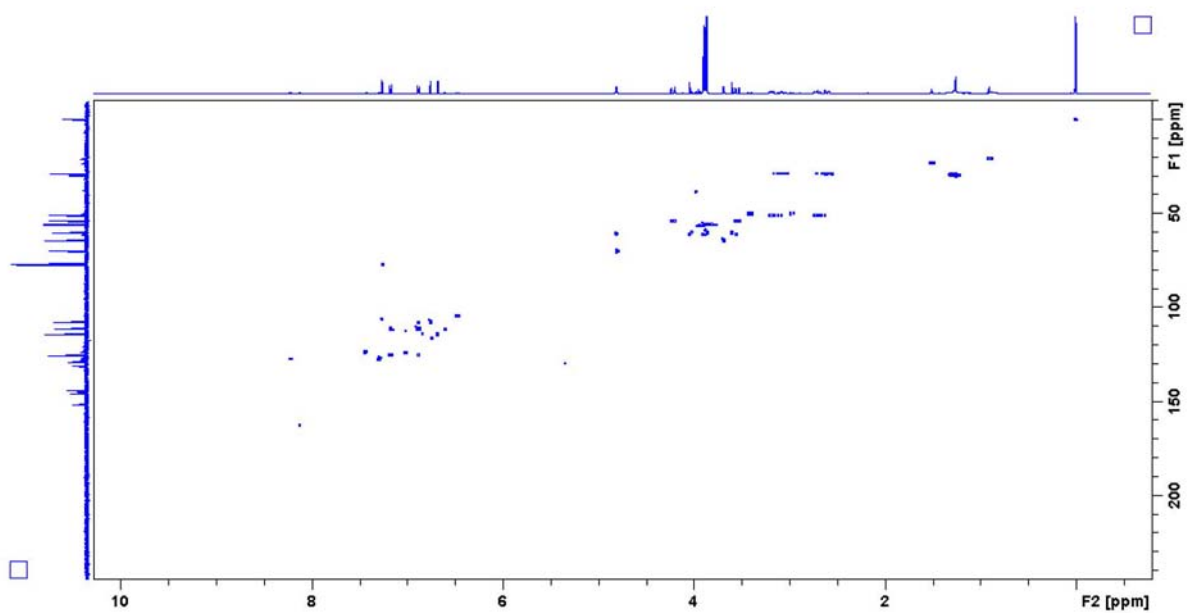


Figure S3. ^1H - ^{13}C one-bond correlation map from HSQC NMR experiment of alkaloid **1** in CDCl_3 at 400 and 100 MHz, respectively.

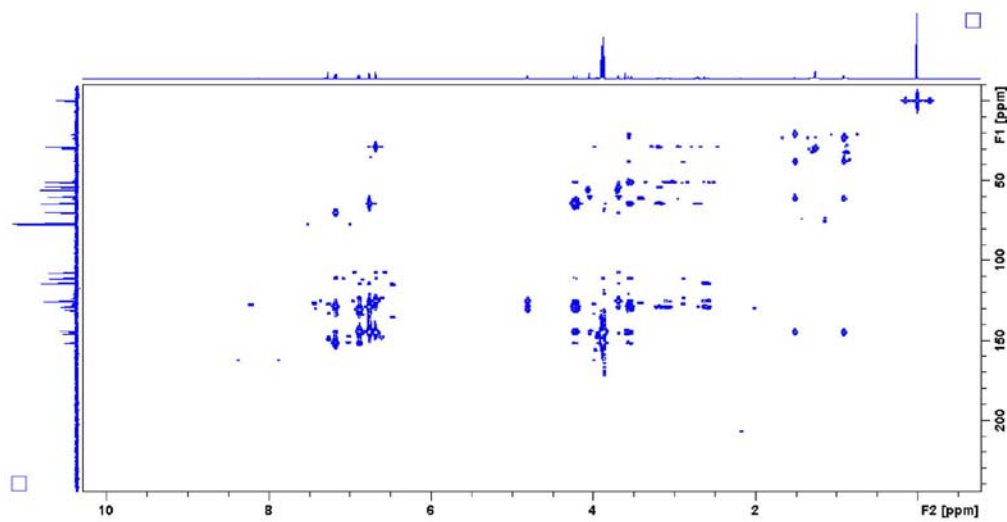


Figure S4. ¹H-¹³C long-range correlation map from HMBC NMR experiment of alkaloid **1** in CDCl₃ at 400 and 100 MHz, respectively.

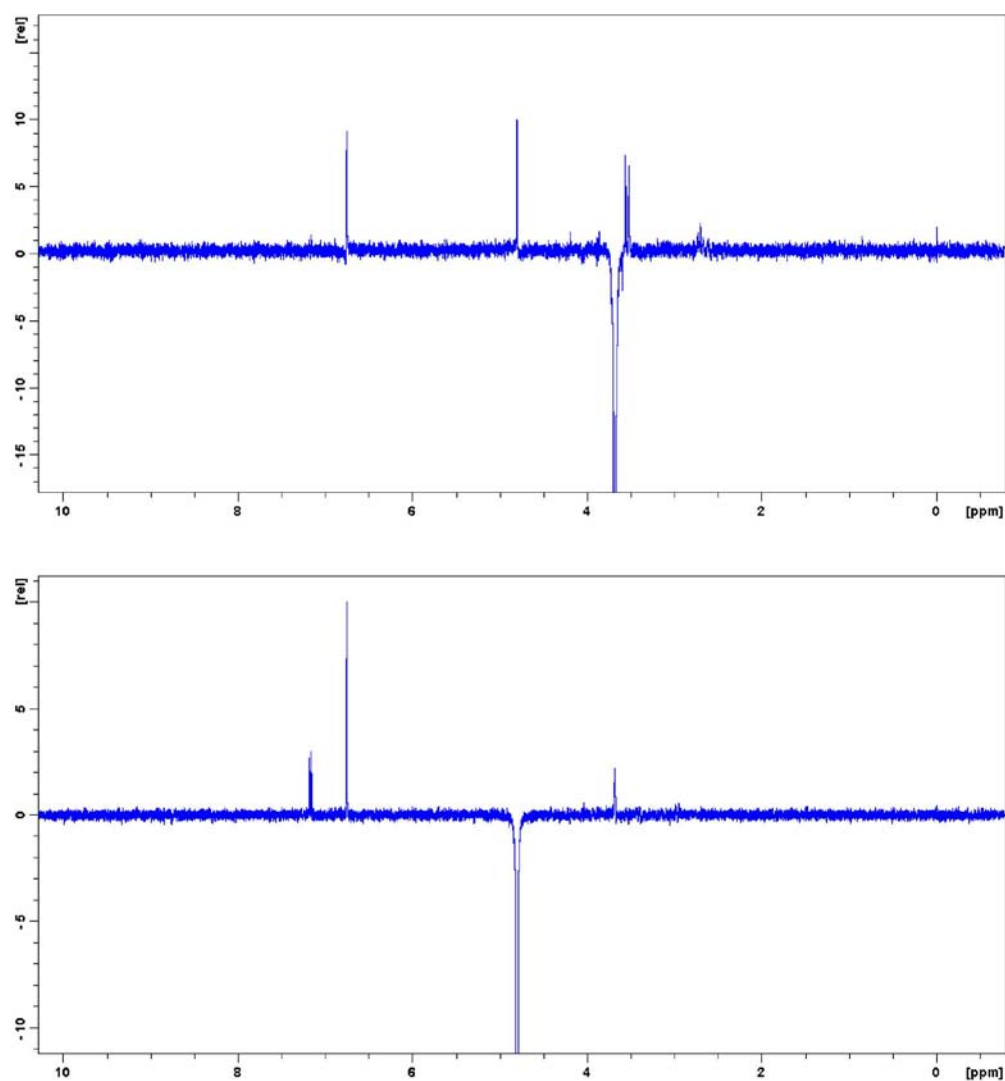


Figure S5. 1D NOE experiments of alkaloid **1** in CDCl₃ at 400 MHz.

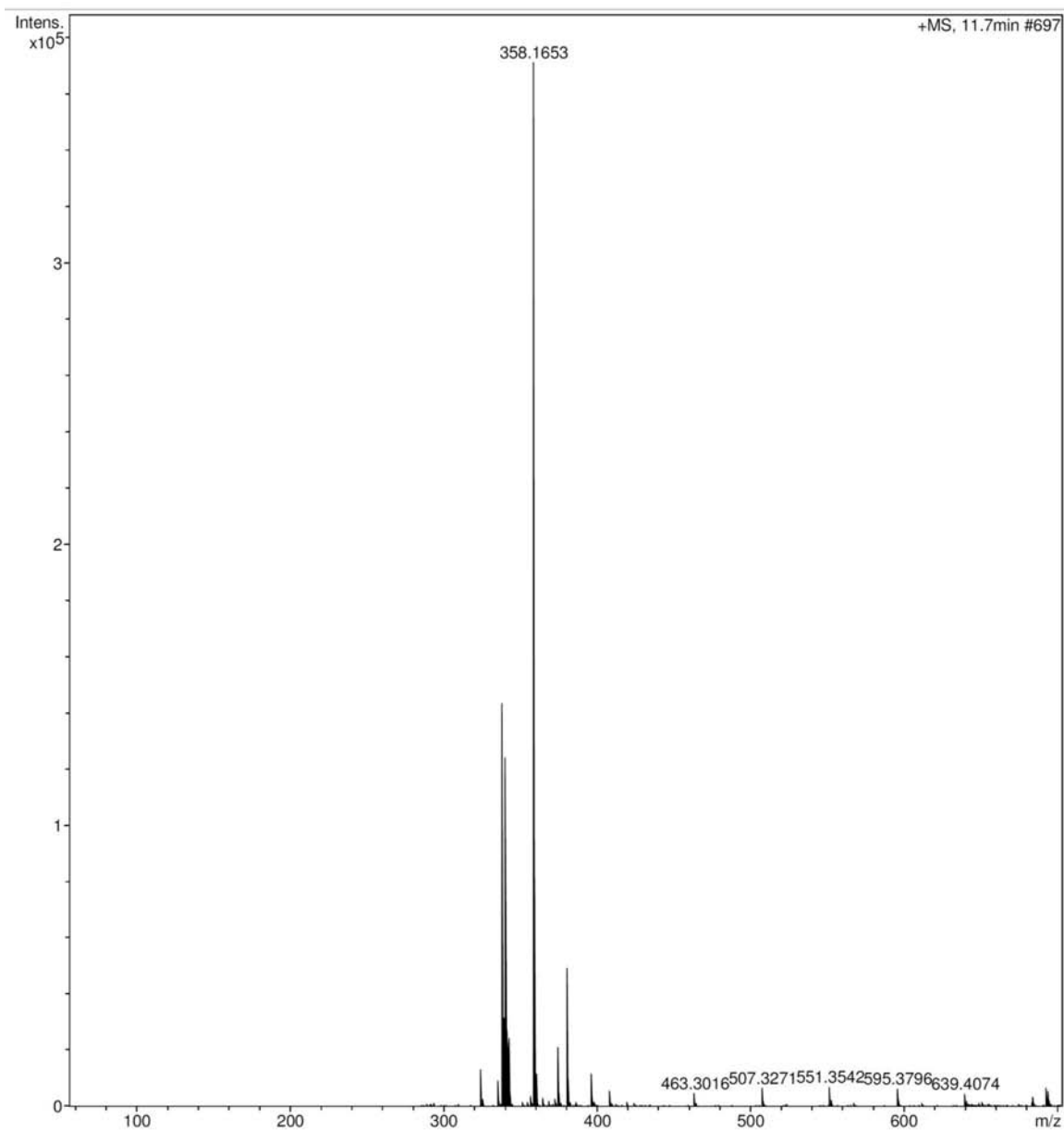


Figure S6. HRESIMS spectrum of alkaloid **1** (m/z 358.1653 $[M + H]^+$).

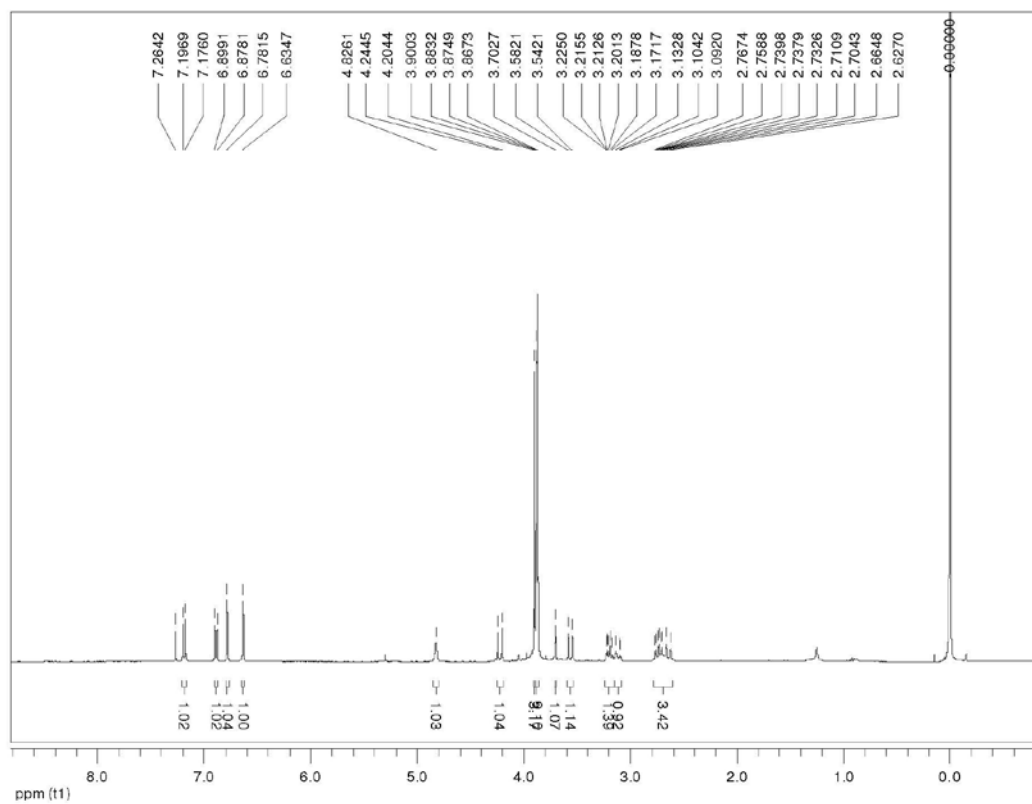


Figure S7. ¹H NMR spectrum of alkaloid **2** in CDCl₃ at 400 MHz.

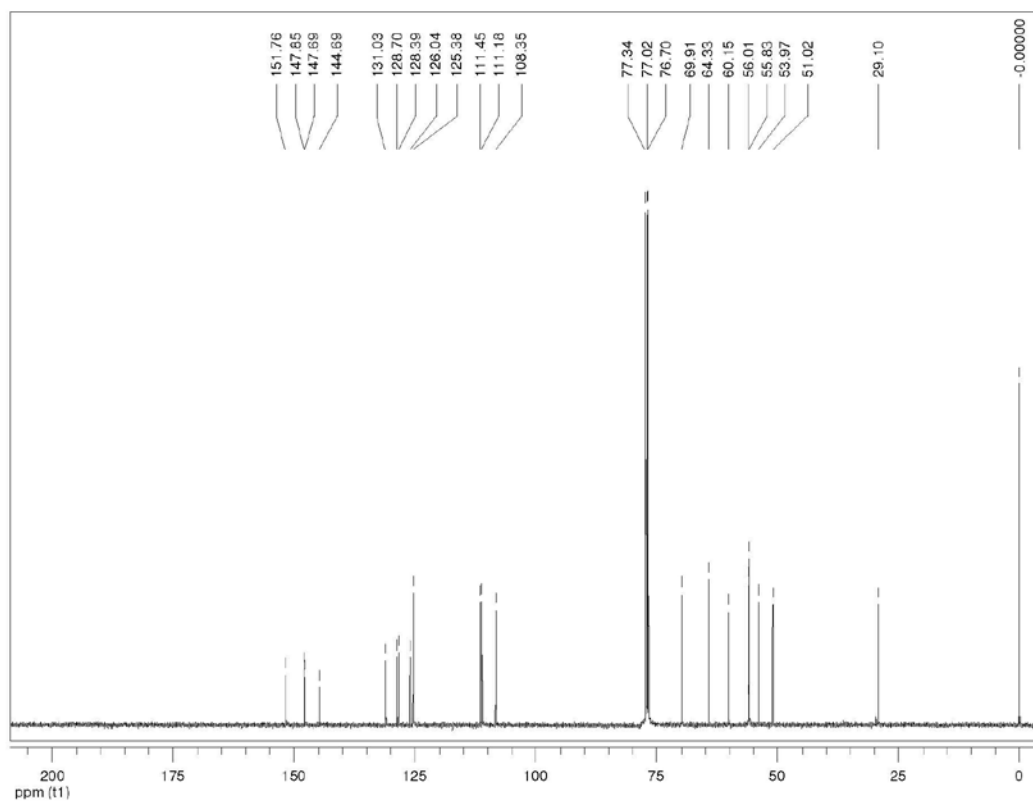


Figure S8. ¹³C{¹H} NMR spectrum of alkaloid **2** in CDCl₃ at 100 MHz.

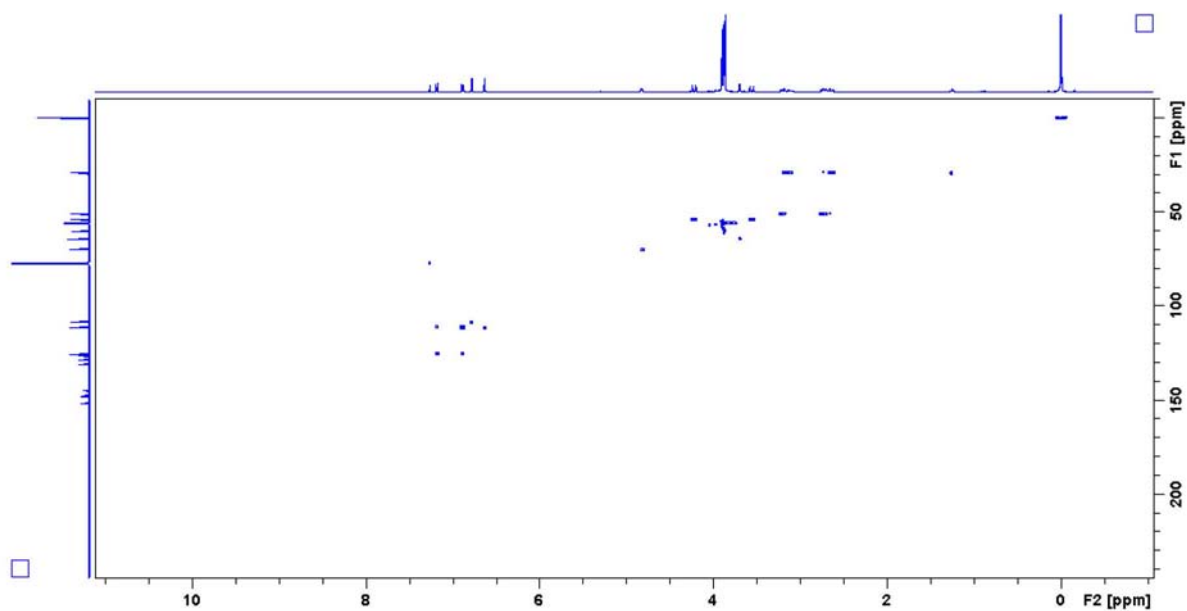


Figure S9. ^1H - ^{13}C one-bond correlation map from HSQC NMR experiment of alkaloid **2** in CDCl_3 at 400 and 100 MHz, respectively.

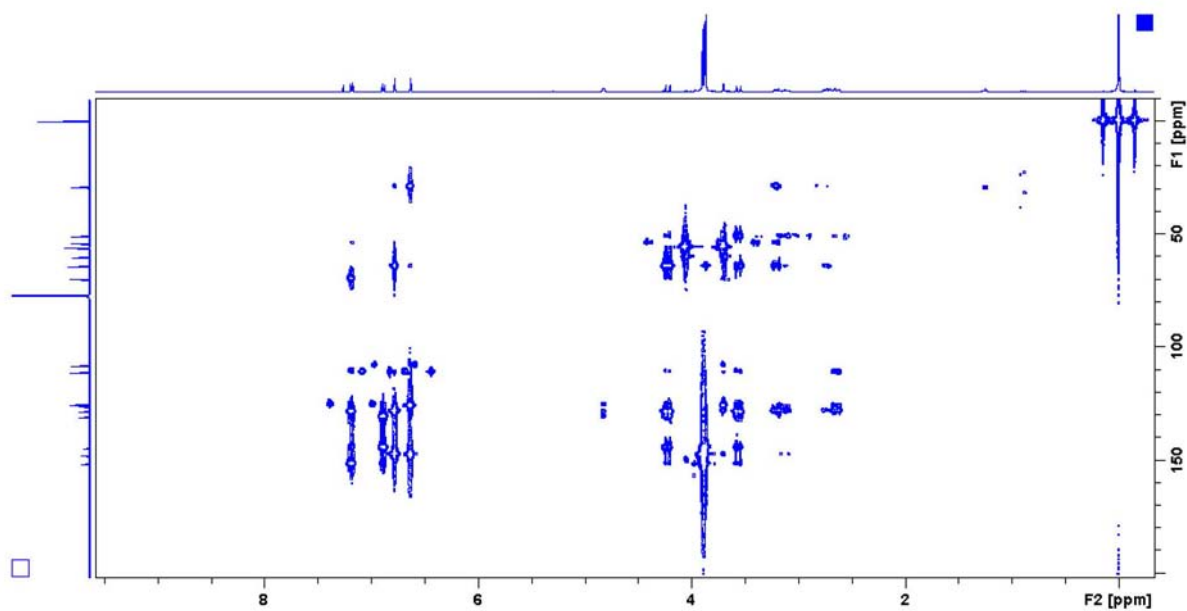


Figure S10. ^1H - ^{13}C long-range correlation map from HMBC NMR experiment of alkaloid **2** in CDCl_3 at 400 and 100 MHz, respectively.

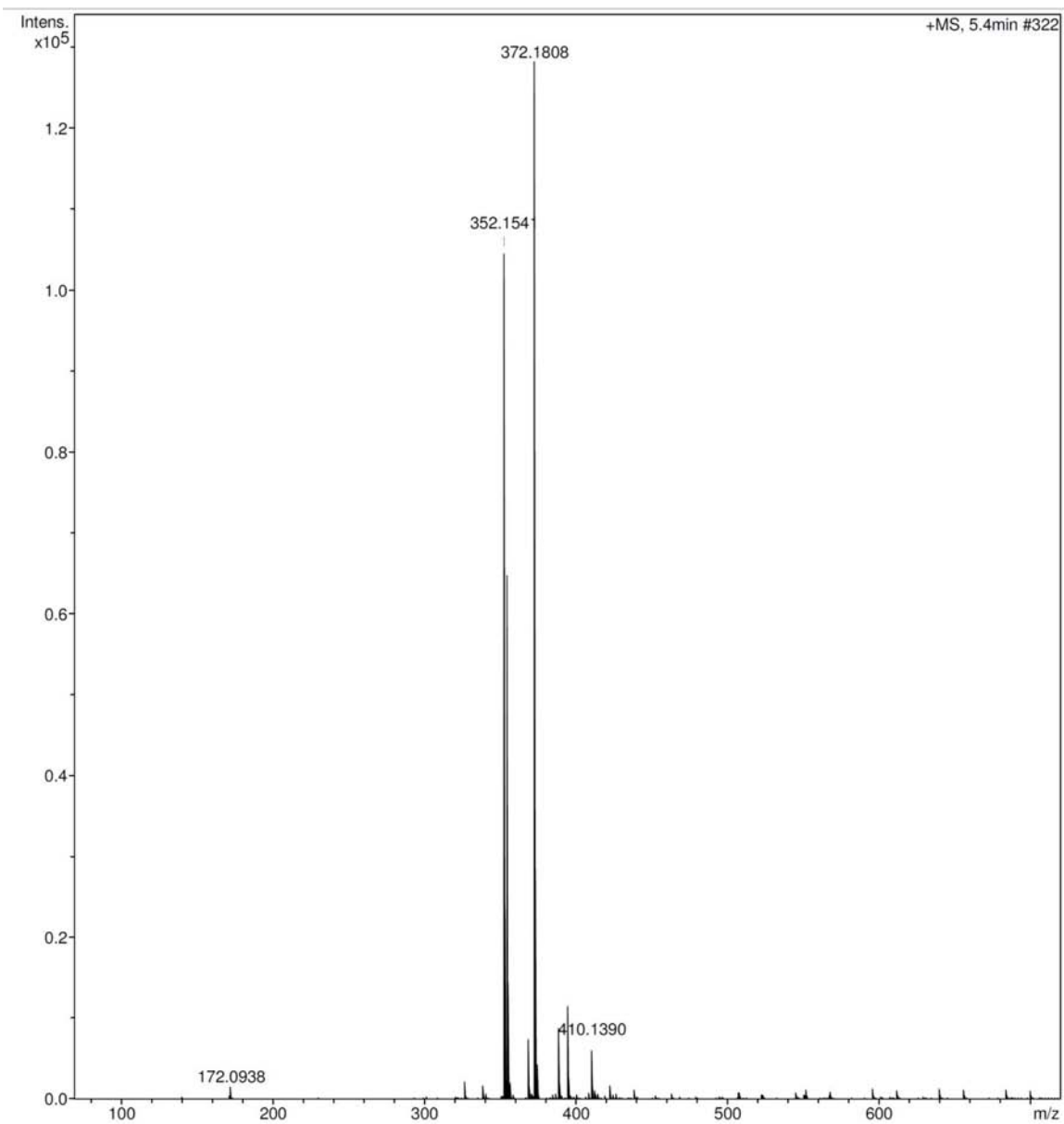


Figure S11. HRESIMS spectrum of alkaloid **2** (m/z 372.1808 $[M + H]^+$).

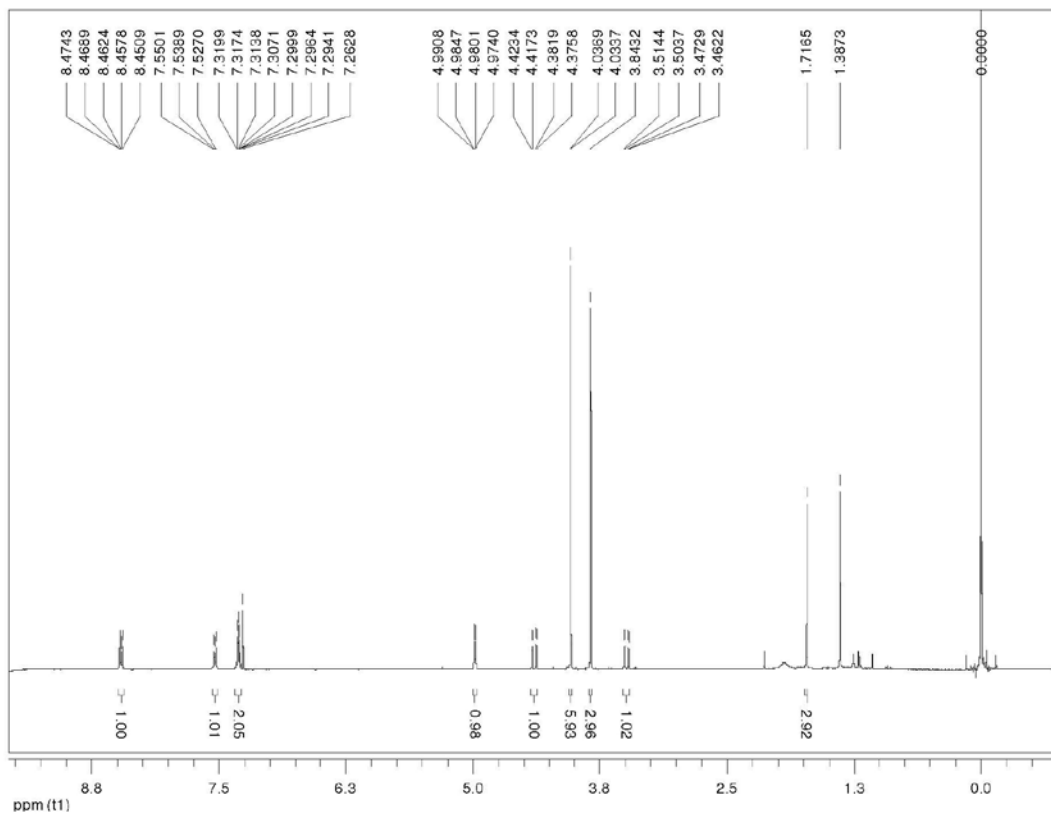


Figure S12. ^1H NMR spectrum of alkaloid **3** in CDCl_3 at 400 MHz.

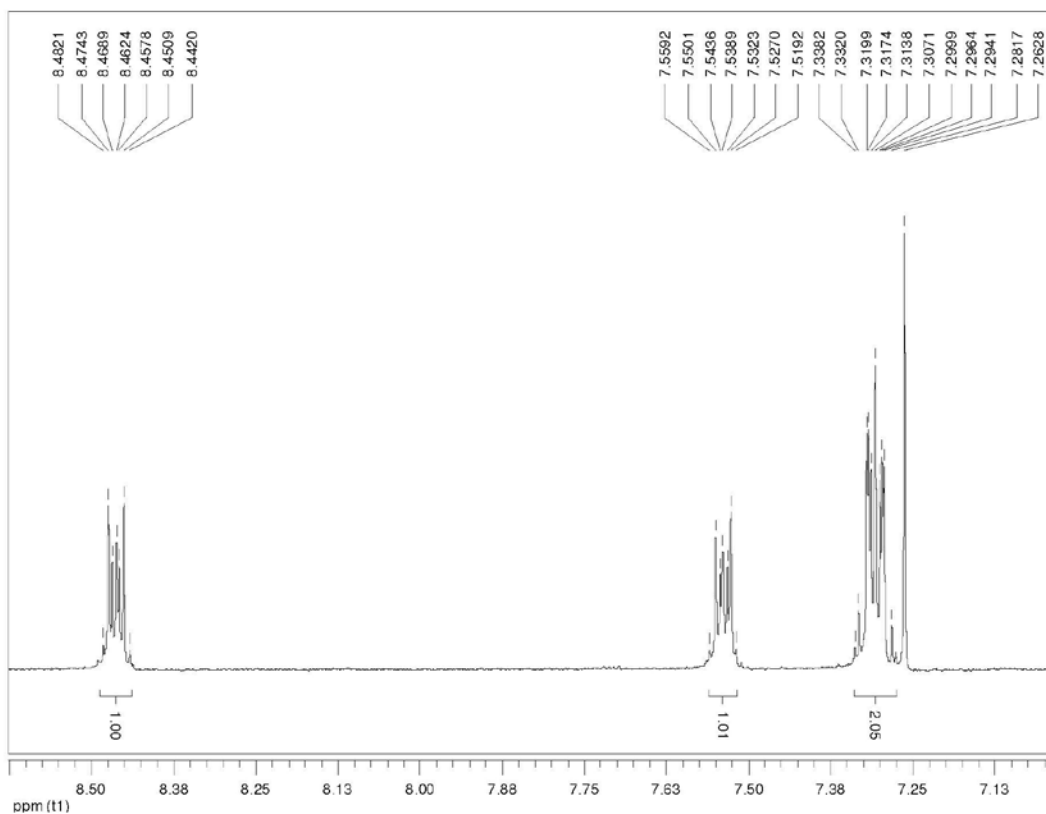


Figure S13. ^1H NMR spectrum of aromatic region of alkaloid **3** in CDCl_3 at 400 MHz.

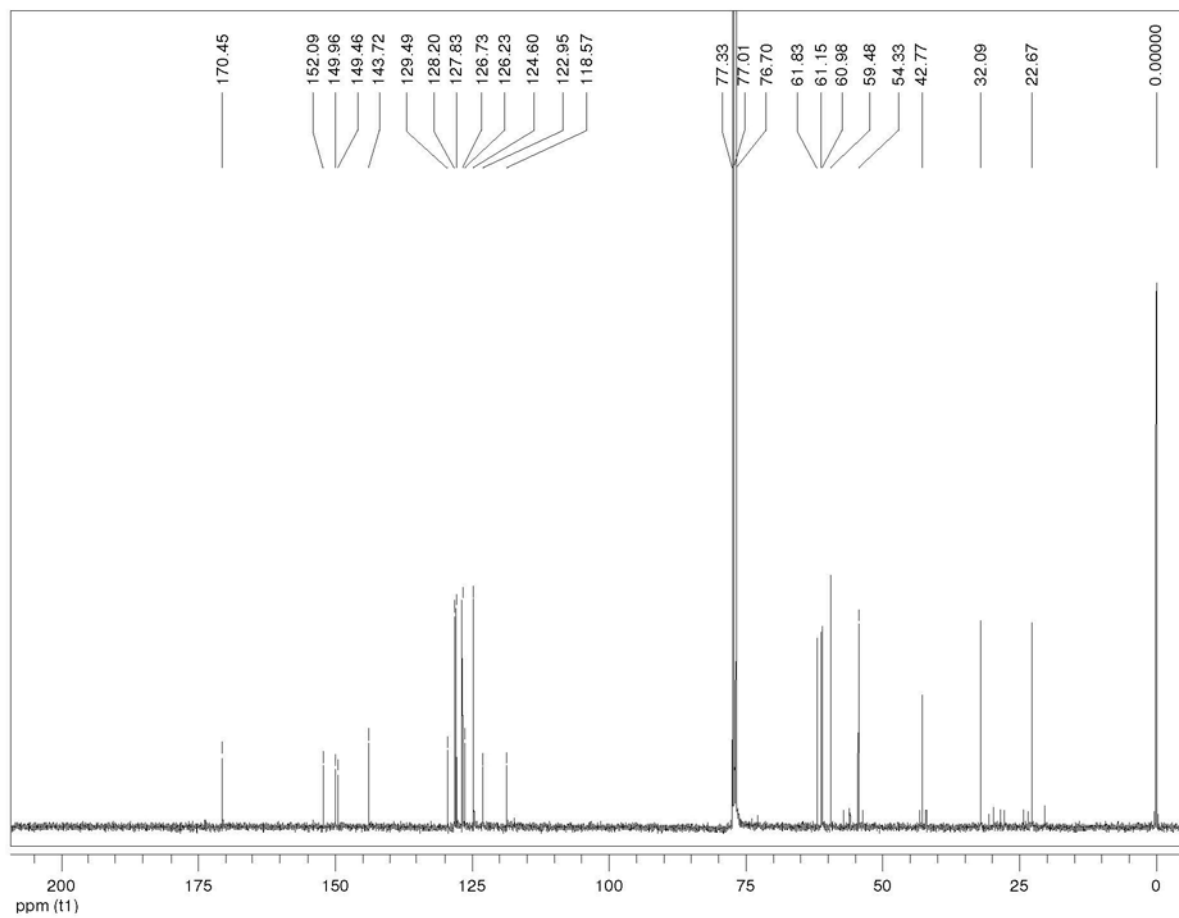


Figure S14. $^{13}\text{C}\{^1\text{H}\}$ NMR spectrum of alkaloid **3** in CDCl_3 at 100 MHz.

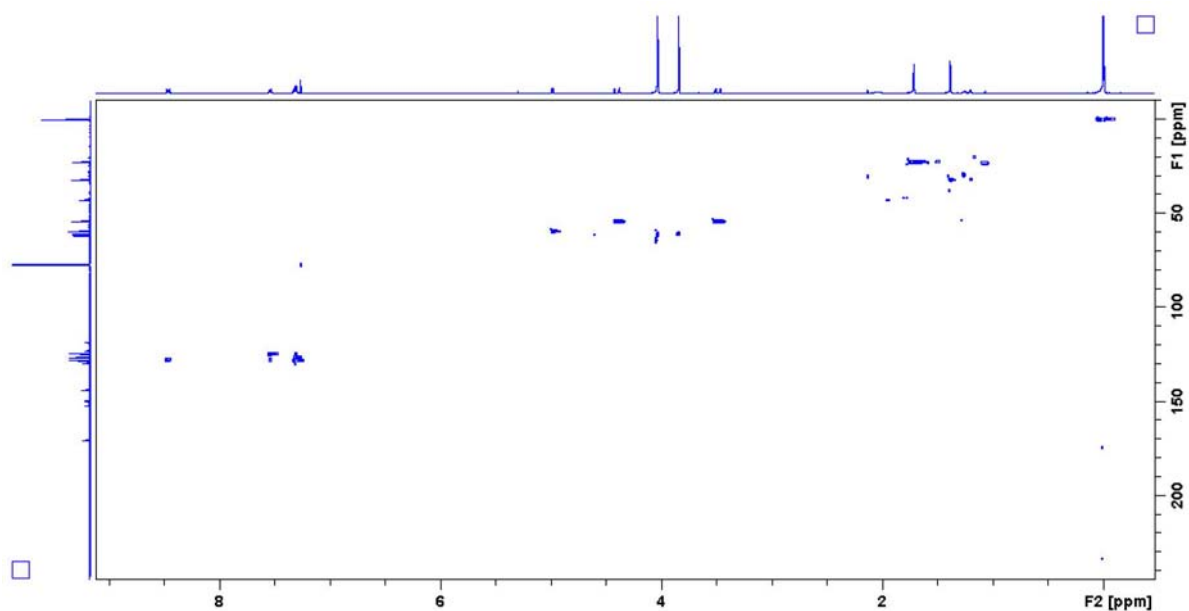


Figure S15. ¹H-¹³C one-bond correlation map from HSQC NMR experiment of alkaloid **3** in CDCl₃ at 400 and 100 MHz, respectively.

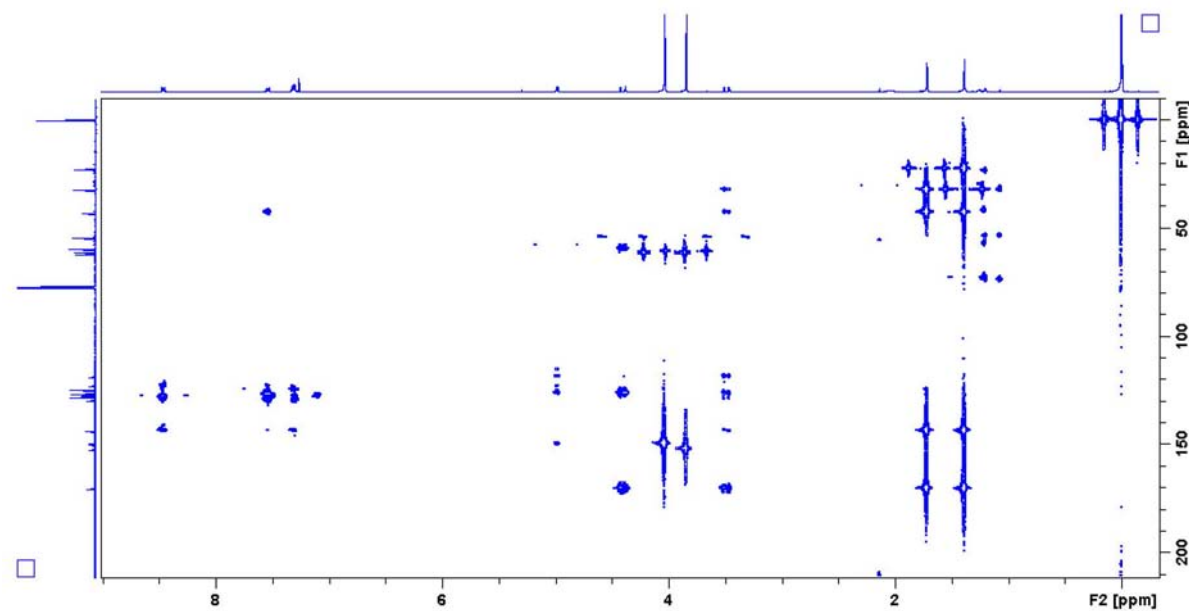


Figure S16. ¹H-¹³C long-range correlation map from HMBC NMR experiment of alkaloid **3** in CDCl₃ at 400 and 100 MHz, respectively.

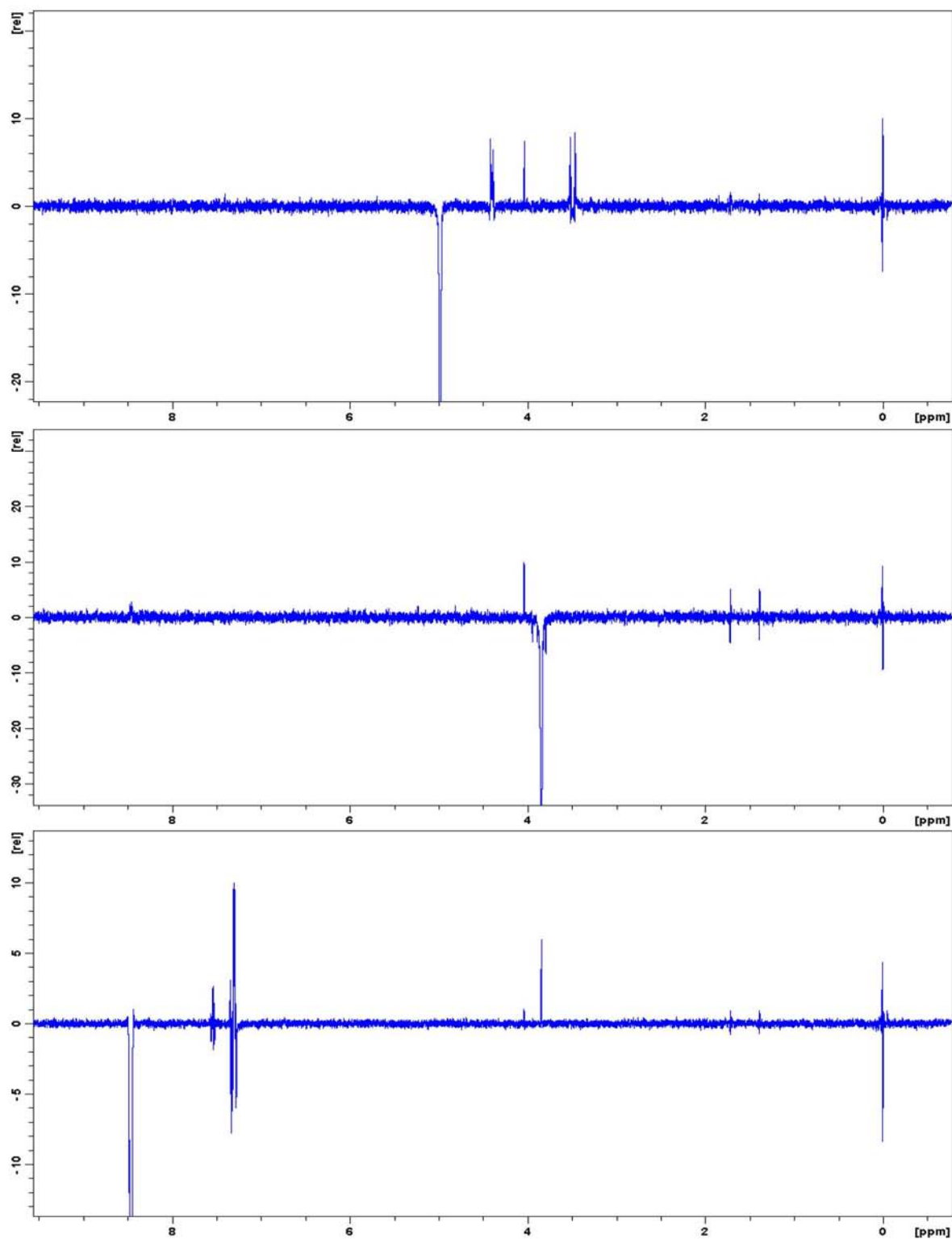


Figure S17. 1D NOE experiments of alkaloid 3 in CDCl₃ at 400 MHz.

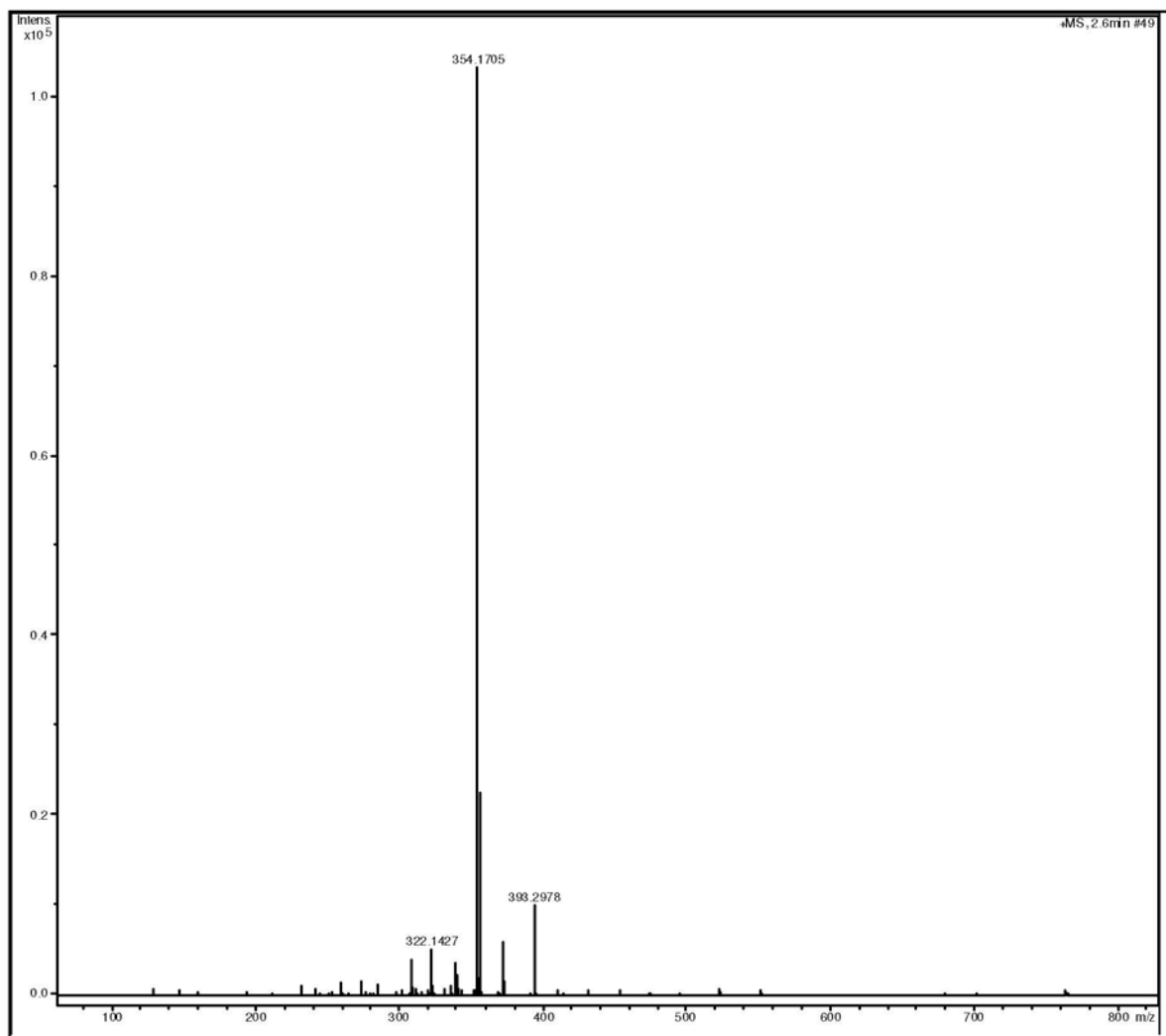


Figure S18. HRESIMS spectrum of alkaloid **3** (m/z 354.1705 $[M + H]^+$).

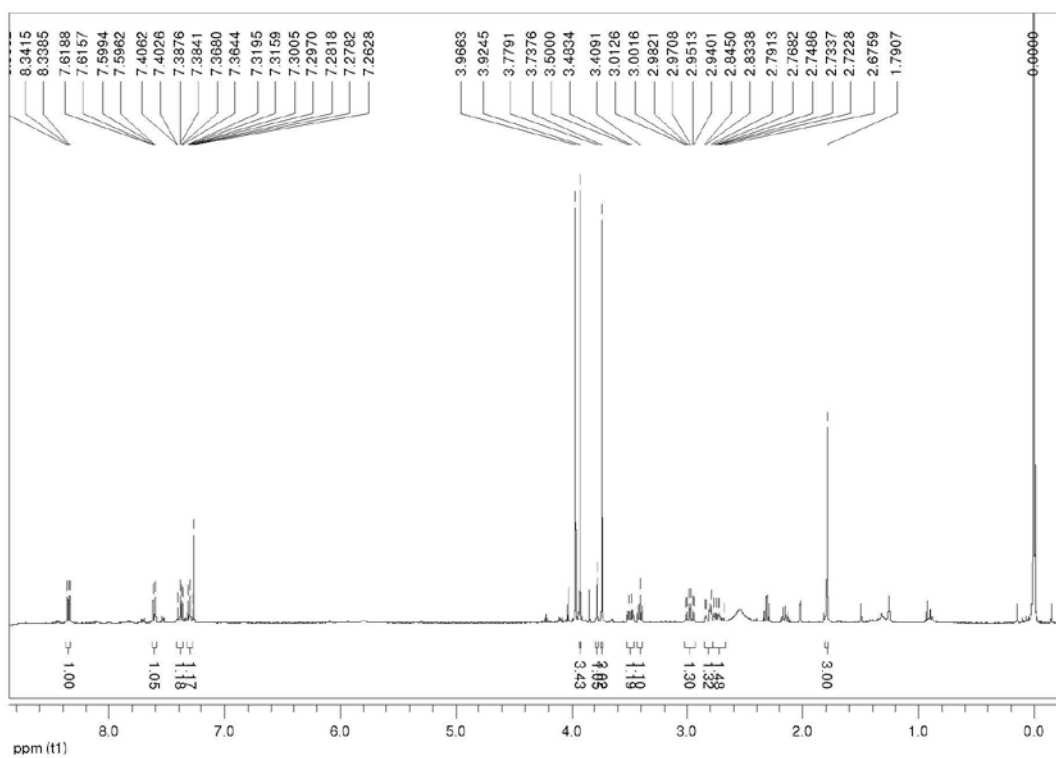


Figure S19. ¹H NMR spectrum of alkaloid 4 in CDCl₃ at 400 MHz.

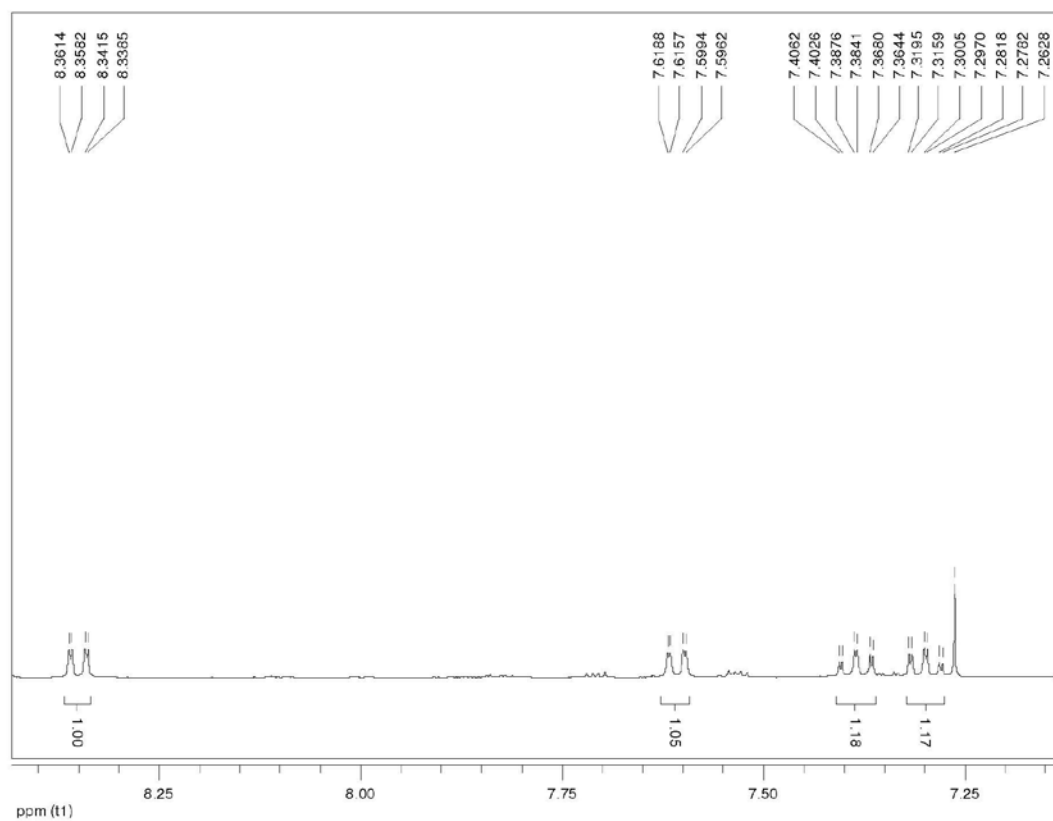


Figure S20. ¹H NMR spectrum of aromatic region of alkaloid 4 in CDCl₃ at 400 MHz.

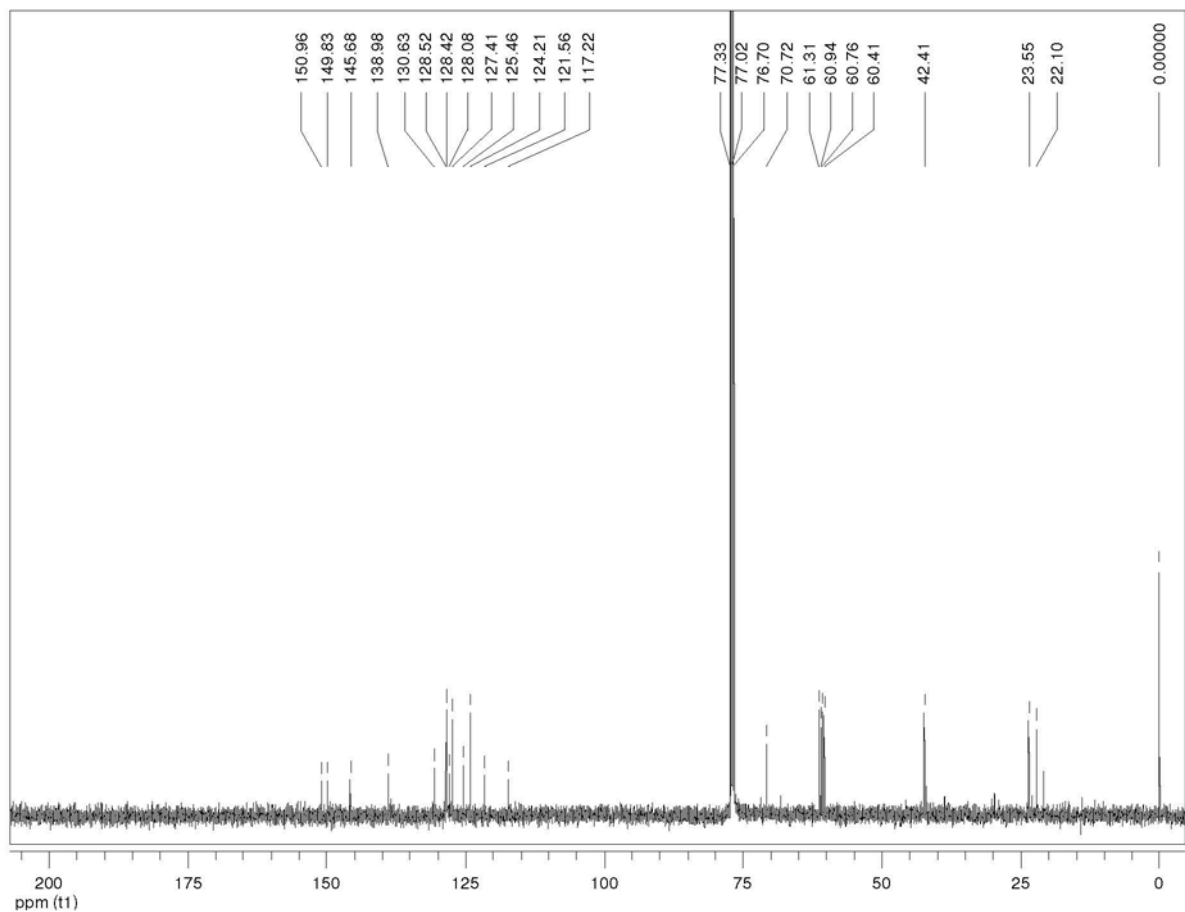


Figure S21. $^{13}\text{C}\{^1\text{H}\}$ NMR spectrum of alkaloid 4 in CDCl_3 at 100 MHz

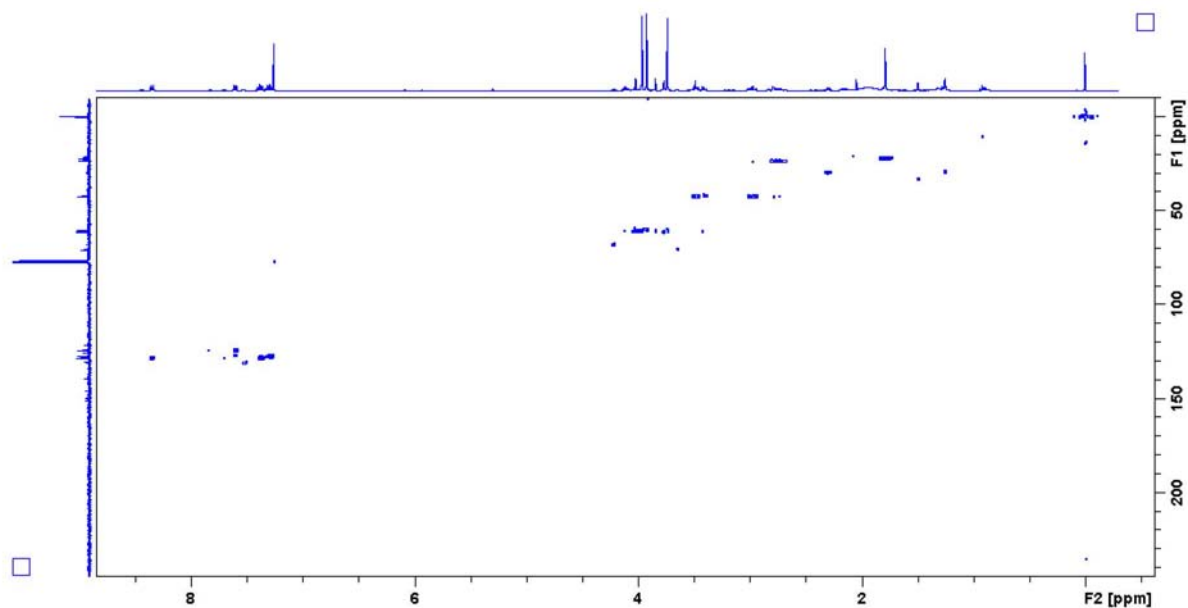


Figure S22. ^1H - ^{13}C one-bond correlation map from HSQC NMR experiment of alkaloid **4** in CDCl_3 at 400 and 100 MHz, respectively.

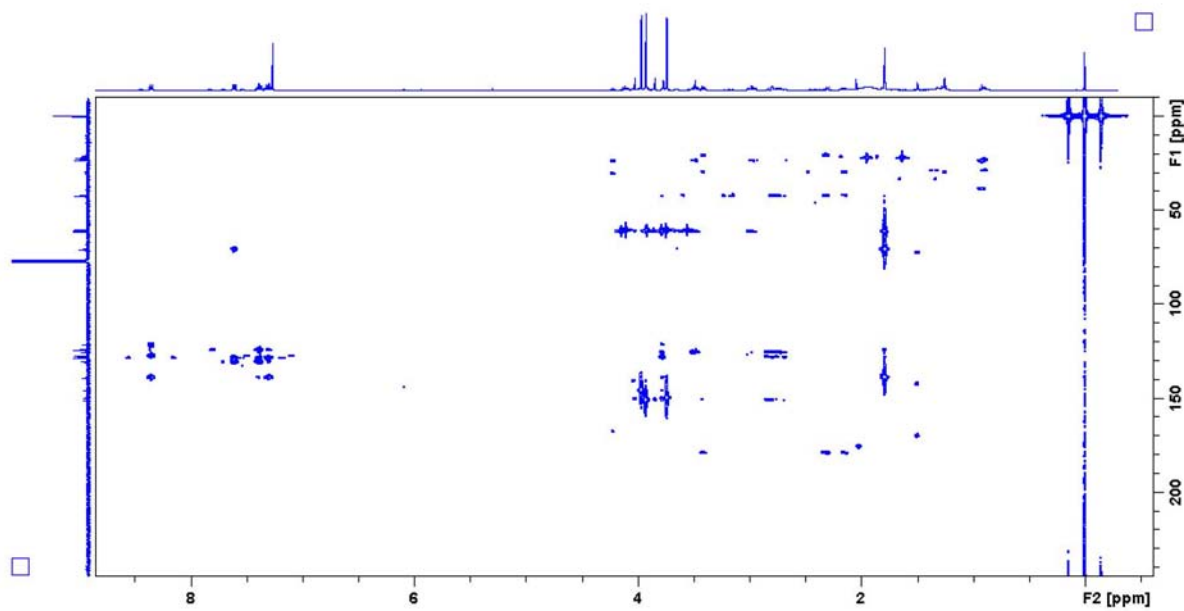


Figure S23. ^1H - ^{13}C long-range correlation map from HMBC NMR experiment of alkaloid **4** in CDCl_3 at 400 and 100 MHz, respectively.

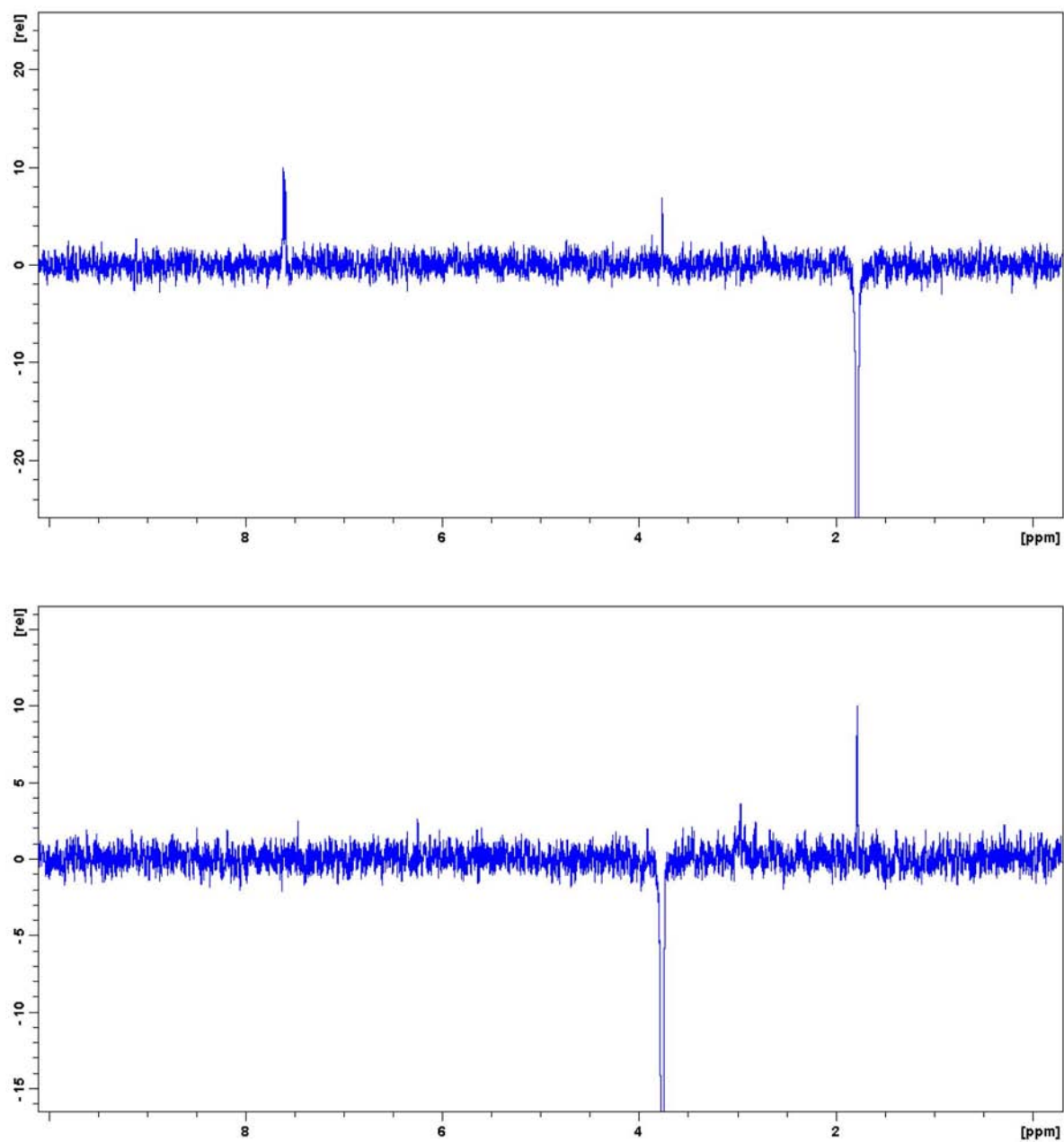


Figure S24. 1D NOE experiments of alkaloid 4 in CDCl₃ at 400 MHz.

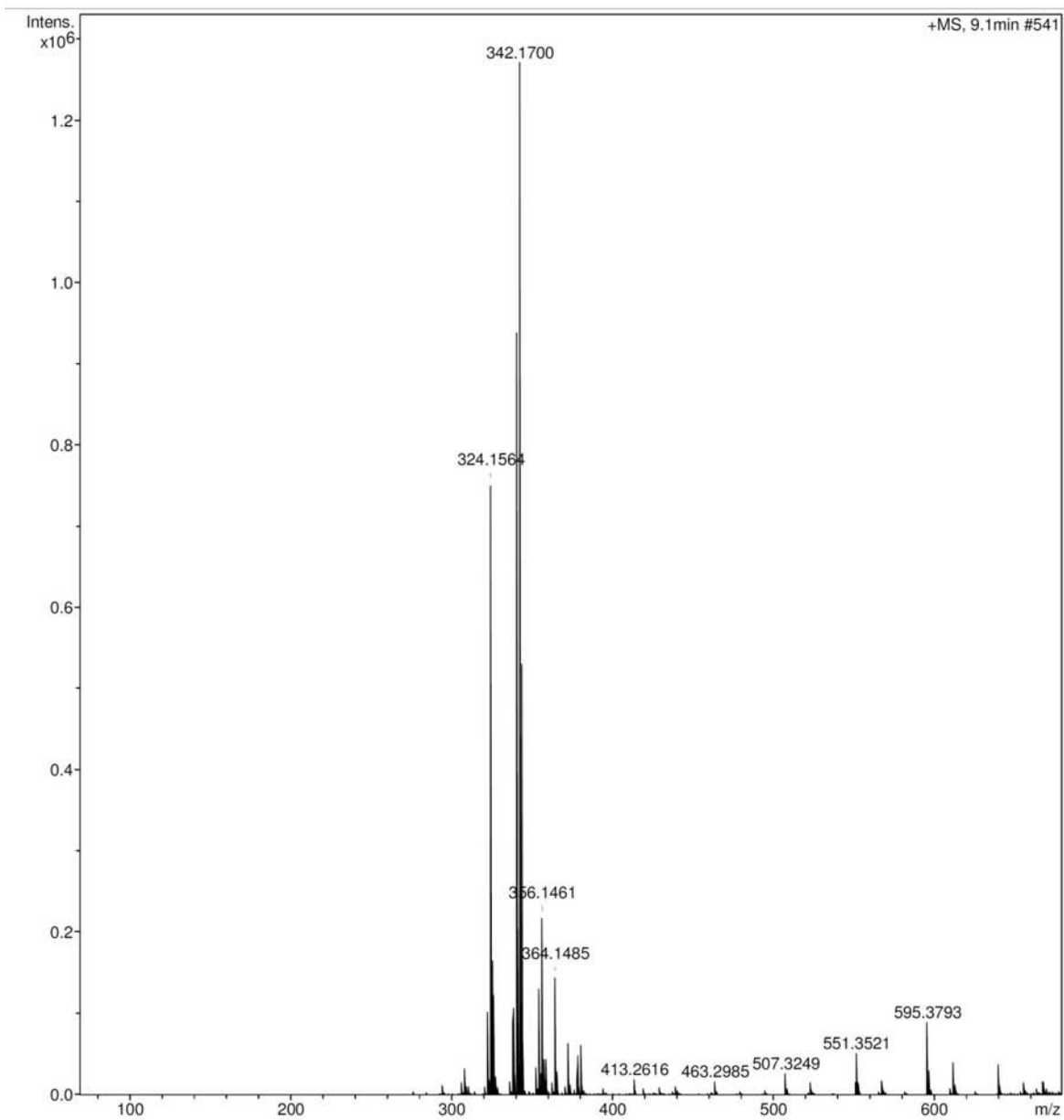


Figure S25. HRESIMS spectrum of alkaloid **4** (m/z 342.1700 $[M + H]^+$).